University of the Witwatersrand

Master of Science in Engineering Degree

An Eco-driving Strategy for an Electric Bus: insert permanent magnet synchronous motor (IPMSM) drivetrain

Author:

Mjozi Robson Jele

Supervisor: Dr. Lesedi M Masisi

A Dissertation submitted to the Faculty of Engineering and Built Environment, University of the Witwatersrand, in partial fulfillment of the requirements for the degree of Master of Science in Engineering.

May 2022

UNIVERSITY OF THE WITWATERSRAND, JOHANNESBURG

Declaration

I, **Mjozi Robson Jele**, declare that this dissertation titled, "**An Eco-driving Strategy for an Electric Bus: insert permanent magnet synchronous motor (IPMSM) drivetrain**" and the contents presented in it are my own unaided work. I confirm that this work was done primarily while I was a candidate for a research degree at the University of Witwatersrand, Johannesburg. I declare that this dissertation is being submitted for the Degree of Master of Science in Engineering at this university. It has never been presented before for any degree or examination at any other University.

Signed: 

Date: 03 May 2022

Abstract

There has been a growing interest in adopting electric vehicles (EVs) over internal combustion engine (ICE) vehicles. However, there are a number of challenges to the adoption of EVs. Firstly, they suffer from low mileage coverage due to poor specific energy in batteries. Secondly, there is a deficit in electric vehicle charging infrastructure and, thirdly, the current battery technology has low charging rates (C-rate). These concerns makes EV to be undesirable as compared to ICE vehicles since gasoline and diesel have high specific energy as compared to batteries. Therefore, it becomes extremely imperative that the onboard finite energy must be used optimally during a driving schedule. This research is concerned with the further development and simulation of an eco-driving strategy for an electric vehicle. This strategy makes use of the vehicle's technical parameters, road gradient, and the electric traction machine efficiency map. A Matlab/Simulink EV model based on an existing EV of the Technical University of Munich (TUM) was developed and validated. The EV model is based on an insert permanent magnet synchronous motor (IPMSM) drivetrain. The EV model was used to develop and validate the eco-driving strategy.

An error of 1.8% in terms of energy consumption for a test drive cycle was observed between the Simulink EV model and TUM EV. Firstly, the TUM EV eco-driving strategy is further developed and simulated by the Simulink EV model. Secondly, the TUM EV is test-driven according to the Simulink EV model simulations. The TUM EV was found to have an optimal speed of 24km/hr for a zero gradient drive route and an error between the energy consumption rates of the Simulink EV model and TUM EV was found to be 1.93%. The TUM EV is found to have an energy saving of 31.2% when driving using the eco-driving strategy. For an acceleration from zero to 24km/hr, the as-fast-as-possible acceleration architecture ($\beta = 0.4$) is found to be 33.33% more efficient as compared to the as-slow-as-possible mode ($\beta = 4$). The eco-drive strategy saves 8.7% for a distance of 550m with a road gradient of 0.076 as compared to conventional driving of an urban eBus. The eco-driving strategy can be applied to any electric vehicle and can be used in conjunction with a GPS navigation system. It can be offered by electric vehicle manufacturers for optimal use of finite battery energy.

I dedicate this research work to the Almighty God my provider

for providing me with the strength and wisdom to research this topic.

I also dedicate this work to my lovely wife Memory Nyasha Chawafambira

for financial, emotional, and other support.

I also dedicate this work to Miss Unathi Jele and Miss Siyamthanda Jele my beautiful daughters

for putting a smile on my face and encouragement during the tough times of this research work.

Acknowledgements

First and most, I would like to thank the Almighty God for the opportunity to research eco-driving strategies for electric vehicles, for the gift of life, for strength and wisdom, for providing me with a helpful supervisor and supportive colleagues in the School of Electrical and Information Engineering (EIE) at the University of the Witwatersrand. I would also like to have a special thanks to my supervisor **Dr. Lesedi M. Masisi** for his mentoring, patience, enlightenment, and dedication throughout this research.

I also like to thank Mr. Robin Geißler and the rest of the Tufast eco-team students from the Technical University of Munich (TUM) for their insightful help in validating the Simulink EV model and the eco-driving strategy. Lastly, but not least, I would also like to acknowledge the National Research Foundation (NRF) for their financial support for this research work.

Contents

List of Figures

List of Tables

Abbreviations

ESS	**E**nergy **S**torage **S**ystem
EV	**E**lectric **V**ehicle
ICE	**I**nternal **C**ombustion **E**ngine
IPMSM	**I**nsert **P**ermanent **S**ynchronous **M**achine
OEM	**O**riginal **E**quipment **M**anufacturer
eBus	**e**lectric **B**us
GHG	**G**reen **H**ouse **G**as
EVCS	**E**lectric **V**ehicle **C**harging **S**tation
IEA	**I**nternational **E**nergy **A**gency
IPMSynRM	**I**nsert **P**ermanent **M**agnet **Syn**chronous **R**eluctance **M**otor
TUM	**T**echnical **U**nirvesity of **M**unich
BEV	**B**attery **E**lectric **V**ehicle
HESS	**H**ybrid **E**nergy **S**torage **S**ystem
IM	**I**nduction **M**otor
NEDC	**N**ew **E**uropean **D**rive **C**ycle
NREL	**N**ational **R**enewable **E**nergy **L**aboratory
LP	**L**inear **P**rogramming
DP	**D**ynamic **P**rogramming
SQP	**S**equential **Q**uadratic **P**rogramming
OCP	**O**ptimal **C**ontrol **P**rogramming
PMP	**P**ontryagin's **M**inimum **P**rinciple
ANN	**A**rtificial **N**eural **N**etwork
COF	**C**oefficient **O**f **F**riction
NCA	**N**ickel **C**obalt **A**luminium
NMC	**N**ickel **M**anganese **C**obalt

LMO	**L**ithium**M**anganese **O**xide
LFP	**L**ithium **I**ron **P**hosphate
LCO	**L**ithium **C**obalt **O**xide
LTO	**L**ithium **T**itanate
TUM	**T**echnical **U**niversity of **M**unich
PSU	**P**ower **S**upply **U**nit
PID	**P**roportional **I**ntegral **D**erivative
TUM EV	**T**echnical **U**niversity of **M**unich **E**lectric **V**ehicle
GPS	**G**lobal **P**ositioning **S**ystem

CHAPTER 1

Introduction

1.1 Introduction

The Paris Agreement of 2015 states that internal combustion engine (ICE) vehicles contribute about 23% of greenhouse gas (GHG) emissions and this is expected to rise to nearly 43% in 2030 and approximately 50% by 2050. To alleviate this trajectory, the International Energy Agency (IEA) advises a growth projection of at least 100 million electric vehicles (EVs) by 2030 [4, 5]. For this reason, mass migration from ICE vehicles to electro-mobility is anticipated. While EV technology has several advantages such as zero to minimal air pollution, EVs also have limitations. The major limitations are: (1) energy storage systems (ESSs) have low specific energy which in turn affects the performance of the EV, i.e., low mileage coverage, (2) there are shortages of electric vehicle charging stations (EVCSs) and (3) the high purchase cost of an EV. Even if the EVCSs are available, the poor charging rate in batteries further exacerbates the problem [6–10]. The aforementioned drawbacks become a challenge for the 2030 demands of the Paris agreement especially in developing and under-developed countries. Alternative methods that have been used to solve the accessibility challenges have included an increase in the battery size which also increases the pricing of the ESSs module while technically increasing the mass of the EV [10]. Other researchers have looked for a traction machine with high efficiency, i.e., the use of an insert permanent magnet synchronous reluctance motor (IPMSynRM), but this, only improves the overall energy consumption rate by 4-10% [2, 11]. Others have investigated automobiles with less weight (carbon fibre) and efficient aerodynamic drag coefficient, however, this only lessens the energy consumption rate by 2-8% [2]. It is for this reason that an energy-saving driving strategy is warranted in order to use the battery energy more effectively. This study aims to develop an eco-driving strategy for electric vehicle applications.

1.2 Problem Statement

More often than not, EV drivers are not aware of an eco-driving strategy at which to drive an EV during a driving schedule so as to optimize the onboard finite energy. This emanates into the traction machine operating at low-efficiency points, thus leading to higher energy consumption and lower energy recuperation. This is particularly prominent for a traction machine with a poor efficiency map propelling an EV with an inefficient aerodynamic drag coefficient (C_d), during a steeper road gradient drive, especially at higher speeds. The traction machine is the main dominant user of the electric energy since it is the only engine of the EV for propulsion. Therefore, if it is inadequately operated, this results in overall inefficient propulsion of the traction machine which results in low mileage coverage per battery charge. Hence, this research proposes an energy-efficient drive strategy to elongate the mileage coverage by the EV. An efficiency map of the traction machine, i.e, IPMSM plus the technical parameters of the EV are employed to come up with the strategy. The methodology in this research does not include the design of the traction motor. Rather, it uses an efficiency map that already exists. There were limitations in terms of available efficiency maps and technical parameters of EVs in general. data

1.3 Research Objectives

This research work aims to develop an energy-efficient driving strategy for an electric bus (eBus) based on an IPMSM powertrain. The research work has the following objectives:

- Develop an EV model based on the IPMSM drivetrain

- Develop and validate an eco-driving strategy
- Develop an eco-driving strategy for an eBus and conduct comparisons with conventional driving

1.4 Research Question

In order to fulfil the objectives of this research work, this work seeks to respond to the following research questions:

- How to formulate an optimal speed driving strategy for an IPMSM drivetrain EV model?
- How to formulate an energy-efficient acceleration strategy for an IPMSM drivetrain EV model?
- What is the energy consumption rate (kWh/km) comparative analysis between eco-driving and conventional driving of an IPMSM drivetrain eBus?

1.5 Research Approach

The major objective of this work is to develop an eco-driving strategy for an eBus. The research approach will be conducted as follows. Firstly, an EV model is developed in Matlab/Simulink. This is done through the usage of longitudinal dynamics and energy consumption equations of the EV. Then, the EV model is validated by means of a drive cycle given to both the EV Simulink model and a real EV. The optimal speed driving and energy-saving acceleration strategies for an EV are developed and validated using a real EV. An eco-driving strategy for an IPMSM drivetrain eBus is then deduced. Lastly, an examination and comparison of drive performances between an eco-driving strategy and conventional driving of the eBus are carried out.

1.6 Dissertation Outline

Chapter 2 surveys the literature concerning the issue of eco-driving in general. It covers the different areas that other researchers have studied in order to improve range anxiety amongst EVs. Chapter 3 looks into the main components that compose the drivetrain of an EV. It further details the most common types of motors and battery technologies that are currently employed by EVs. Chapter 4 covers the development and implementation of the EV model in Matlab/Simulink. Chapter 5 deals with the development of the eco-driving driving strategy. This involves both an optimal speed driving algorithm and an energy-efficient acceleration strategy. Chapter 6 applies the eco-driving strategy to an IPMSM propelled eBus and discusses and analyzes the results. Chapter 7 is the conclusion of the research work and the possibility of future work.

1.7 Dissertation Contributions

1.7.1 Chapter 4

An EV model is designed and implemented using Matlab/Simulink software. The model considers the vehicle parameters, longitudinal dynamic equations, and motor energy equations. Drive cycle simulations of the Simulink EV model give the motor shaft torque and speed. These operating points are then utilized to obtain the efficiency points on the efficiency map which is then used to calculate the energy consumption from the battery. Energy consumption characteristics can be associated with the forces which act on the EV. The model is then validated against a real EV that was developed by students from the University of Munich (TUM) for their 2019 Shell Eco-marathon Competition. This whole process is done by following the Waterfall model-based design. Unfortunately, the model is unable to capture and account for all the energy consumption from the battery.

1.7.2 Chapter 5

The model that was developed and validated in chapter 4 is employed to formulate an eco-driving strategy for EVs. The strategy encompasses both optimal speed driving and an energy-efficient acceleration. The algorithm needs the technical parameters of the EV, the efficiency map of the traction machine, and the elevation profile of the drive route. This is used to compute the motor torque and speed which is then used to acquire the efficiency on the efficiency map of the traction machine. Thus, the energy consumption from the battery is calculated. Both strategies are then validated by using the real EV.

1.7.3 Chapter 6

Application of the eco-driving strategy on an eBus by means of simulations is executed. The strategy is applied on an eBus in order to estimate energy consumption and possible energy savings during drive schedules. This could then be used to estimate its battery size and to determine if the transmission and distribution system has enough capability to sustain the bus energy requirements. This is done for both urban and extra-urban driving on inter-campus routes. A comparison between eco-driving versus convectional driving is carried out.

1.8 List of Publications

1.8.1 Conference Paper Published

Mjozi Jele and Lesedi Masisi. An Eco-driving Strategy for an Electric Bus: IPMSM drivetrain. In *2021 IECON, 47th Annual Conference of the IEEE Industrial Electronics Society(IES)*, pages 1–6, 2021. [Student, first author: Partial conceptualization, paper write up, designed the simulation set up, conducted simulations and analysis of results. Supervisor, second author: Conceptualization of the idea of the paper, the structure of the paper, paper editing and supervision]

CHAPTER 2

Literature review

2.1 Introduction

The issue of mileage anxiety in EVs has prompted different researchers to look amongst others into the following: ESS, efficiency improvement of the drive-line components, dynamic EV charging, vehicle body, powertrain configurations, and energy-efficient drive strategies. These are summarised as shown in the tree diagram in Fig. 2.1.

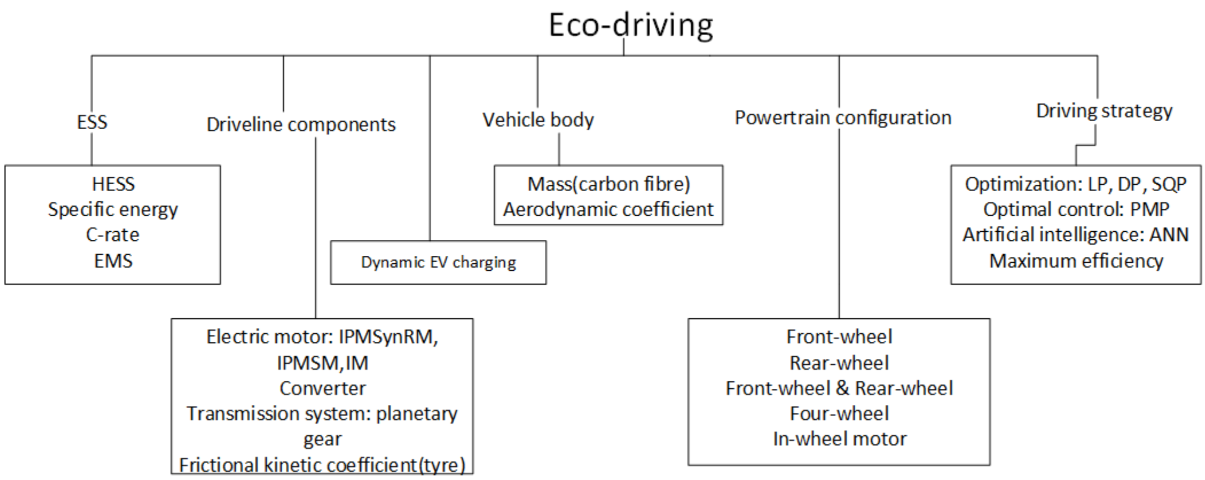

Figure 2.1: Elements of eco-driving

2.2 Eco-driving

Batteries have a very high specific energy but low C-rate yet super-capacitors are the exact opposite. So many researchers and energy experts have turned into the quest for a hybrid energy storage system (HESS) that encompasses both technologies. A HESS has the following advantages: (1) enhances vehicle acceleration, (2) increases the driving range, (3) extends the battery life cycle, (4) decreases the capital cost by replacing expensive batteries, and (5) has high specific energy and high C-rate [12–14]. In the pursuit of a best-performance motor, [11] compares the IPMSM to the insert permanent magnet synchronous reluctance motor (IPMSynRM). The IPMSynRM (ferrite-assisted) is found to be 25% cheaper than the insert permanent magnet synchronous motor (IPMSM) but competitive with it in terms of torque, torque-speed performance, power factor, and efficiency. [15] concludes that the IPMSM and the induction motor (IM) have unique efficiency maps: at lower speeds and low-medium torque levels, the IPMSM was found to be 4% higher in terms of efficiency than IM. But at higher speeds and lower torque levels, the reverse held true. Thus the study then suggests that an IM/IPMSM powertrain configuration would be superior in EVs since it can either extend the range or lessen the battery size for a certain fixed range. [9, 16] explores dynamic electric vehicle charging systems on the roads. Such a system charges the battery while the EV is in motion thus reducing the onboard battery size and solving the problem of mileage anxiety.

[17] builds up an EV prototype that is autonomously driven by four in-wheel motors. The torque values and efficiency maps are investigated for both the motoring and regenerative modes in experiments performed on a chassis dynamometer. The outcomes suggest an improvement in the overall operational efficiency of the EV. [18] interrogates a torque distribution characterization for a front-wheel and rear-wheel driven EV. It was concluded that maximum efficiency is attained if the total torque requirements of the vehicle are equally distributed by two identical motors. Additionally, an energy consumption analysis was performed over the New European drive cycle (NEDC) whereby the low-torque and high-speed regions were seen

to consume more energy. Thus, therefore, it would be crucial to improve the motor efficiency in these regions. It was also found that the drivetrain efficiency could be improved by a clutch between the motor and gearbox. [19] studied a model-based mileage extension control system for an EV propelled with four in-wheel motors. The slip ratio and copper and iron losses of the motors are enhanced corresponding to vehicle velocity and acceleration over the Japanese JC08 drive cycle. It was found that the system can elongate the mileage coverage and precisely determine energy consumption.

[20] The National Renewable Energy Laboratory (NREL) studies the driving styles of ICE vehicles so as to save on fuel usage in the US. It observes that in spite of not altering the drivetrain of the vehicle, but the removal of stop-and-go driving and needless idling, changing acceleration rates and cruising velocities to optimal levels could lead to energy consumption rate savings of more than 30%. Nevertheless, this is largely subject to vehicular automation and traffic flow. [21] defines eco-driving as key decisions (vehicle choice and care), deliberate decisions (path selection and vehicle mass), and driving style which decreases fuel consumption rate. The study concludes that all these factors can amass to about 45% in fuel economy. Some of the well-known energy-efficient driving strategies usually employ optimization and optimal control techniques, i.e, linear programming (LP), dynamic programming (DP), sequential quadratic programming (SQP), and Pontryagin's Minimum Principle (PMP) [22]. These techniques consider the driving mission as an optimal control problem (OCP) and resolve it to come up with an optimal velocity trajectory that the vehicle follows such that it minimizes its energy consumption rates. In [6] LP works out the longitudinal dynamics of an ICE haulage truck to compute its velocity trajectory for a known road topology. The results show fuel savings of about 3-4% on highway driving and even more on steep slopes. DP is also engaged to select an optimal gear profile for the truck since it is known to be good with discrete problems. [23] comes up with an eco-driving assistance system to lower the usage of energy in EVs. An EV model is developed and the OCP is resolved using DP to produce an energy-efficient velocity profile. [24] presents an algorithm that reformulates eco-driving by avoiding the

introduction of additional non-convex variables. SQP is engaged to solve the optimal control problem. [22, 25] presents an optimization method for energy-efficient driving in EVs. This algorithm develops steady-state solutions with the application of PMP necessary conditions by considering the driving schedule as an OCP. Disturbances and restrictions to the system, as a result of road gradients, speed limits, safety, etc were treated and converted to interior-point boundary conditions of the problem. This energy-saving driving strategy is found to save between 4.3% and 43.6% energy as compared to conventional driving. The authors in [7] use an artificial neural network (ANN) to propose a model-based strategy that projects and optimizes the energy usage for a driving schedule before it commences. An optimal velocity profile is determined and provided to advise the driver during the trip. This driving strategy considers vehicle dynamics, road gradients, and real-time traffic conditions. The study in [26] looks into the advantages of using a two-speed gearbox to enhance EV energy efficiency. The outcomes reveal that it is feasible to increase energy efficiency with a two-speed gearbox but it greatly relies on the motor efficiency map. [2] develops an energy-efficient driving strategy to save energy for a fully electric bus in Xi'an. A full electric bus model composed of the longitudinal dynamics, electric motor, battery, and accessories modules were built in AVL CRUISE software. This driving strategy is referred to as the maximum motor efficiency technique. The velocity of 40km/hr was found to have less energy consumption rate (kWh/km), thus yielding more range. But the driver was advised to vary between 30-40 km/hr velocity as much as possible depending on traffic conditions and safety. The acceleration characteristics β of EV were also scrutinized. It was found that the convex acceleration approach $(0 < \beta < 1)$ expends less energy as compared to the concave acceleration approach $(1 < \beta < \infty)$. Specifically, $(0.2 < \beta < 1)$ was established as the acceleration characteristic parameter with a lesser kWh/km for this eBus.

This study aims to develop an eco-driving strategy for an IPMSM-based EV in order to optimize battery energy usage which thus extends mileage coverage. It closely follows the study in [2].

2.3 Summary

This chapter reviewed the different elements of eco-driving which had been studied by different authors in recent years. These studies were attempts to resolve the issue of mileage coverage by EVs which is the biggest barrier to EVs into the mainstream market. This chapter mainly consisted of how certain drive-line components can be optimized so that they expend less energy during the EV operation. On-board charging devices and dynamic charging roads were also covered. Lastly, energy-saving driving techniques that are employed to drive the EV so as to optimize the electrical battery energy usage were also surveyed.

CHAPTER 3

Background

3.1 Introduction

Energy consumption of an EV depends on the following factors: mass, rotational mass coefficient, gravitational acceleration, kinetic coefficient of friction, road gradient, aerodynamic drag coefficient, frontal area, vehicle velocity, vehicle acceleration, headwind velocity, air density, transmission system efficiency, wheel radius, gear ratio, motor efficiency, time and battery efficiency (superimposed with converter efficiency). These factors are mainly divided into three types. Firstly, there are those factors that the EV original equipment manufacturer (OEM) can choose and/or manipulate during the design stage of the vehicle. This mainly depends on the type and class of the vehicle. These include among others the mass, rotational mass coefficient, kinetic coefficient of friction, aerodynamic drag coefficient, frontal area, transmission system efficiency, wheel radius, gear ratio, motor efficiency, time, and battery efficiency. Secondly, there are those factors that are nature and weather conditions dependent i.e air density, road gradient, headwind velocity, gravitational acceleration. Lastly, there are those factors that the EV driver can be able to control during the EV operation, i.e, vehicle velocity and acceleration.

In this research work, transmission efficiency and battery efficiency are assumed to be very high and constant. Motor efficiency is a function of motor speed and torque and its provided by the efficiency map of the traction machine. Gravitational acceleration is assumed to be 9.81m/s^2. Headwind velocity is neglected. The following subsections give more details on these factors and their influence on EV energy consumption.

3.2 Vehicle Dynamics

Fig. 3.1 shows all the longitudinal forces that act on the EV model during motion. Unlike, the ISO8555/DIN7000 orientation which considers the lateral and vertical forces as well, this model considers the longitudinal forces only.

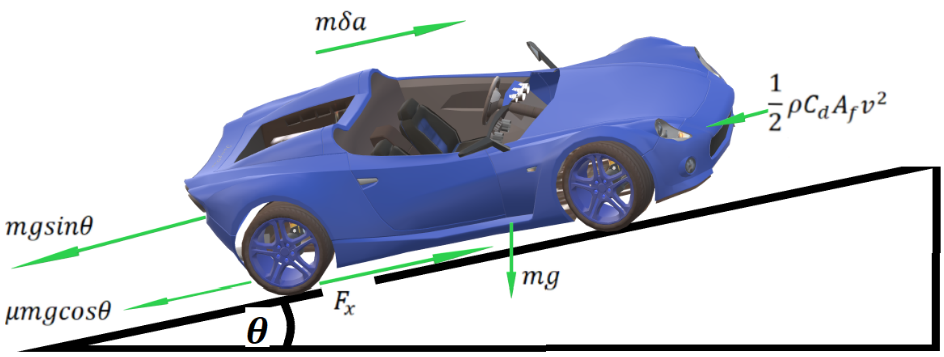

Figure 3.1: Electric vehicle force diagram

The acceleration force F_a, which is a resultant force that must overcome all the other forces in order for the vehicle to get into motion is given by:

$$F_a = m\delta a \tag{3.1}$$

where m is the mass of the EV in kg, δ is the rotational mass coefficient and a is the acceleration of the vehicle in m/s^2. The kinetic frictional force F_k is a force that acts between the tires and the road is given by:

$$F_k = \mu mg\cos\theta \tag{3.2}$$

where μ is the kinetic coefficient of friction, g gravitational acceleration constant and θ is the road gradient. The hill-climbing force F_c is a force that acts against or enhances vehicle motion depending on whether the vehicle climbs and descends a slope, respectively, is given by:

$$F_c = mg\sin\theta \tag{3.3}$$

The aerodynamic drag force F_d is a force that pushes on the frontal area of the vehicle as it moves through the fluid air is given by:

$$F_d = \frac{1}{2}\rho C_d A_f (v + v_0)^2 \tag{3.4}$$

where ρ is the air density, C_d is the drag coefficient, A_f is the frontal area of the vehicle, v is the longitudinal velocity of the vehicle in m/s, v_0 is the headwind in m/s (assumed to be zero in this research). Newton's law of motion stipulates that, for the EV to start driving, the acceleration force must overcome all the other forces shown in Fig. 3.1 [2, 22, 25]. Therefore, the traction force F_x, on the wheels of the EV is described by:

$$F_x = m\delta a + \mu mg\cos\theta + mg\sin\theta + \frac{1}{2}\rho C_d A_f (v + v_0)^2 \tag{3.5}$$

The torque demand from the electric motor is calculated as:

$$\begin{aligned} T_m &= \left(\frac{F_x}{\eta_T}\right)\left(\frac{r_w}{n_d}\right) \\ &= \frac{m\delta a + \mu mg\cos\theta + mg\sin\theta + \frac{1}{2}\rho C_d A_f (v + v_0)^2}{\eta_T}\left(\frac{r_w}{n_d}\right) \end{aligned} \tag{3.6}$$

where η_T is the transmission efficiency, r_w is the wheel radius and n_d is the transmission ratio. The motor shaft angular speed ω, in rad/s, is derived from the vehicle's longitudinal velocity v, is given as:

$$\omega = n_d \left(\frac{v}{r_w} \right) \tag{3.7}$$

The motor shaft speed N, in revolutions per minute (rpm), is derived from ω as follows:

$$N = \omega \left(\frac{60}{2\pi} \right) \tag{3.8}$$

The power on the shaft of the motor is given by:

$$P_m = \omega T_m \tag{3.9}$$

The mechanical shaft motoring energy E_M and the mechanical shaft generating energy E_G are calculated, respectively as:

$$E_M = \int_0^t P_m dt \tag{3.10}$$

$$E_G = -\int_0^t P_m dt \tag{3.11}$$

The energy consumption from the battery during motoring can be calculated as follows:

$$E_{motor} = \frac{E_M}{\eta_b} \tag{3.12}$$

where n_b is the battery efficiency plus converter efficiency. The energy that get stored in the battery during regenerative braking can be calculated as follows:

$$E_{gen} = \eta_b E_G \tag{3.13}$$

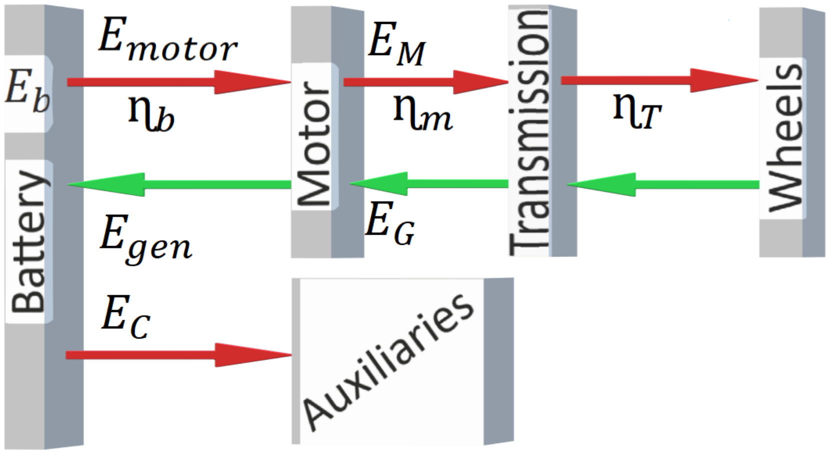

Figure 3.2: Motoring/regeneration energy flow

Energy flow has two directions as shown in Fig. 3.2. During motoring, energy flows from the battery to energise the motor which then propels the transmission system to drive the wheels. This is depicted by the red arrow in Fig. 3.2. During regenerative braking, energy in the wheels propels the transmission system. Then, the transmission system drives the traction motor to generate energy which gets stored in the battery. This is shown by the green arrow in Fig. 3.2. During the motoring mode, the battery energy, E_b, can be calculated as follows:

$$\begin{aligned} E_b &= \frac{1}{\eta_b}\left(E_c + \frac{E_M}{\eta_m \eta_T}\right) \\ &= \int_0^t \frac{v}{\eta_b}\left(E_c + \frac{m\delta a + \mu m g \cos\theta + m g \sin\theta + \frac{1}{2}\rho C_d A_f (v + v_0)^2}{\eta_m \eta_T}\right) dt \end{aligned} \tag{3.14}$$

where η_m is the motor efficiency provided by the efficiency map, η_b and E_c is the energy consumed by auxiliaries.

3.2.1 Drive cycle

An automotive drive cycle is the time-velocity profile of the vehicle during a driving schedule which also shows the driver's behaviour. It is used for vehicle simulations in order to analyze how the performance of the vehicle i.e energy consumption, maximum speed, maximum acceleration. Fig. 3.3 shows an example of a drive cycle, the US06 drive cycle which is predominantly characterized by high acceleration styles.

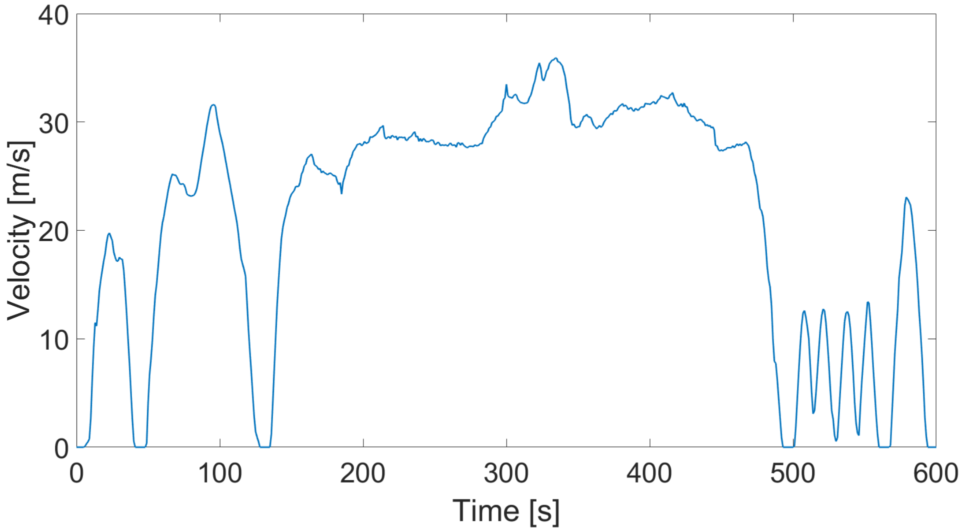

Figure 3.3: US06 drive cycle

3.2.2 Efficiency map of the traction machine

This is a speed-torque contour chart that depicts the ratio of the output mechanical energy to the input electrical energy or vice-versa of the traction machine. It has speed(rpm) on the x-axis and torque(Nm) on the y-axis. Fig. 3.4 shows an example of an IPMSM efficiency map that was generated using Motor-CAD, a known EV simulator software. The blue points are the speed-torque operating points that were generated for a bus drive cycle simulation. If these operating points fall on a low-efficiency point the energy consumption from the battery increases. For consumption to be minimum, the speed-torque points of the drive cycle must coincide with the high-efficiency contours.

3.2.3 EV Technical Parameters

a. Vehicle Mass and Rotational Mass Coefficient δ

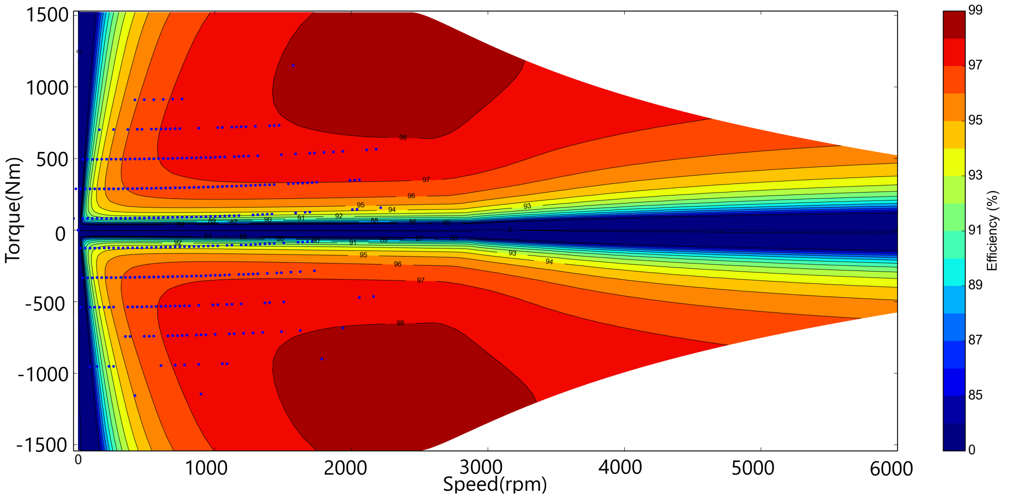

Figure 3.4: Example of an efficiency map

Mass is the number of particles that are there in an object and kg is the SI unit. It's a physical property of the object that quantifies its resistance towards acceleration or deceleration which is called inertia according to Newton's first law. The higher the mass of a vehicle, the higher the amount of acceleration force required to get it into motion, thus, more energy is required as depicted by equations 3.1 and 3.14 [2, 27]. Mass is also directly proportional to F_r and F_c. This means that a vehicle with a lot of mass requires more energy for its motion.

Interestingly, the force F_a does not only depend on the mass of the vehicle only but also on the masses of the rotating parts in the vehicle i.e engine, transmission system, wheels, flywheel, crankshaft. Hence, the multiplication with δ, the rotational mass coefficient to account for all the rotational masses in equation 3.1. δ can be calculated as follows:

$$\delta = 1 + \delta_s + \delta_k \tag{3.15}$$

where δ_s is a constant for a given car and it can be calculated as

$$\delta_s = n_d^2 \frac{I_g^2 I_s \eta_b}{r_w^2 m} \tag{3.16}$$

and δ_k is calculated as

$$\delta_k = \frac{4I_k}{r_w^2 m} \tag{3.17}$$

where m is vehicle gross mass, n_d is transmission ratio, I_g final drive ratio, η_b is transmission system efficiency, I_s is engine rotating parts mass moment of inertia, I_k is wheel mass moment of inertia and r_w wheel radius.

δ can also be simplified as

$$\delta = 1 + \frac{m_e}{m} \tag{3.18}$$

where m_e is the total of all the masses that are rotating on the drive-line.

b. Aerodynamic Coefficients (drag C_d and lift C_l)

There is a continual demand for excellent fuel economy, higher vehicle performance, lowering of wind noise levels and advanced road holding and stability for vehicles in motion. This has accelerated vehicle OEMs to research further on drag and lift aerodynamics for different body shapes operating in different ambiances. The aerodynamic drag coefficient, C_d, is a dimensionless number that gives a measure of the resistance of the vehicle body as it traverses through the viscous air. A higher, C_d, hinders the vehicle acceleration and leads to higher energy consumption, especially at higher speeds. C_d is as a subsequent pressure build-up between the front and rear of the vehicle as shown by the green arrows in Fig. 3.5. Thus, the rear and front surface area shapes of the vehicle have a significant effect on the C_d value.

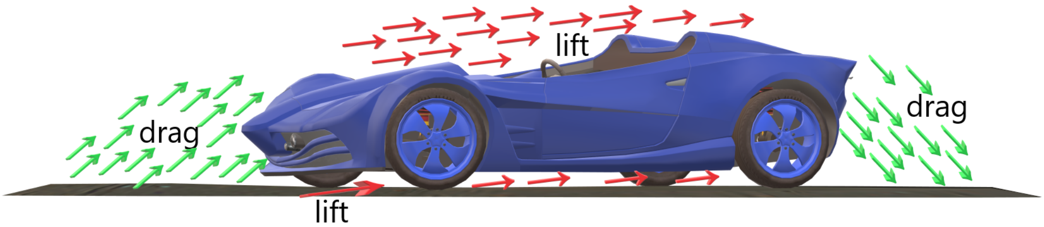

Figure 3.5: Vehicle body aerodynamics: drag and lift

Likewise, the aerodynamic lift coefficient, C_l, is a dimensionless number that gives a measure of the resistance of the vehicle's body which results from pressure build-up above and below the vehicle's body as it traverses through the viscous air. This is illustrated by the red arrows in Fig. 3.5. Consequently, this develops upward (positive lift) and downward (negative lift) forces.

$$F_l = \frac{1}{2}\rho C_l A_f v^2 \tag{3.19}$$

where C_l lift coefficient. The upward force is undesirable as it attempts to veer off the vehicle from the road while the downforce reinforces the road holding capability of the vehicle [3, 28]. The vehicle length plays a very crucial role in C_d. Ideally, a longer vehicle has a smaller C_d, since it causes the airflow around the vehicle body to delay in splitting [28]. The vehicle OEMs in Formula 1, dedicate a lot of time and millions of dollars to perfect the front wing end-plate which increases the downward force. This makes the car turn corners at great speeds. Normally, the $\frac{C_l}{C_d}$ ratio is 2.5 [29]. Table 3.1 shows drag coefficients of different vehicle classes.

Table 3.1: Vehicle type and their drag coefficient [3]

vehicle type	drag coefficient (C_d)
Saloon car	0.22 - 0.4
Sports car	0.28 - 0.4
Light Van	0.35 - 0.5
Buses and Coaches	0.4 - 0.8
Articulated trucks	0.55 - 0.08
Ridged truck and bar trailer	0.7 - 0.9

c. Frontal Area (A_f)

This is the surface area of the vehicle which is perpendicular to the air flows. The drag force, F_d is directly proportional to A_f as already demonstrated by equation3.4. For a similar reference area and matching Mach number and Reynolds number, an airfoil (teardrop) shape in Fig. 3.6 has the lowest C_d as compared to other shapes [29–31].

d. Air Density ρ

Figure 3.6: Airfoil shape has the smallest C_d

This is the mass per unit volume of atmospheric air measured in $[kg/m^3]$. According to the International Standard Atmosphere (ISA) at $15°C$ and sea level, the air density is $1.225kg/m^3$. This is a mere approximate value as air density depends on pressure, temperature, and the amount of water vapor in the air. For example at $20°C$ and 101.325 kPa, $\rho = 1.2041kg/m^3$. Air density also depends on altitude. The higher the altitude, the air density becomes dense [32].

e. Coefficient of Friction (COF)

The coefficient of friction is a dimensionless ratio of the frictional force, F_s or F_r, that opposes the movement between two bodies and the normal force F_N. COF is divided into two kinds: static COF, μ_s for stationary bodies, and kinetic COF, μ_k for relative movement between bodies. These can be defined by the following equations [33]:

$$\mu_s = \frac{F_s}{F_N} \tag{3.20}$$

and

$$\mu_k = \frac{F_k}{F_N} \tag{3.21}$$

where

$$F_N = mg \tag{3.22}$$

and this is subject to

$$F_s > F_k \tag{3.23}$$

In vehicles, μ_k contributes about 20% of energy consumption in cars and small trucks. Michelin Urban Concept tire with $\mu_k = 0.00013$ and Michelin Energy Saver+ tire with $\mu_k = 0.008$ are one of the most energy-efficient tires [34].

3.3 Battery Electric Vehicle (BEV) Drivetrain Technology

A BEV is a zero-emission vehicle propelled by an electric motor that is energized by a battery through a power converter. Fig. 3.7 shows the general layout of all the main components in an EV powertrain. It consists of an on-board charger, a battery pack, auxiliaries, power electronics converter, electric motor, transmission system, and wheels. The electric motor and power converter are integrated into an electric drive system. The EV drivetrain is similar to that of an ICE vehicle, except that the fuel tank and the engine are replaced with the battery pack and electric drive system, respectively [35].

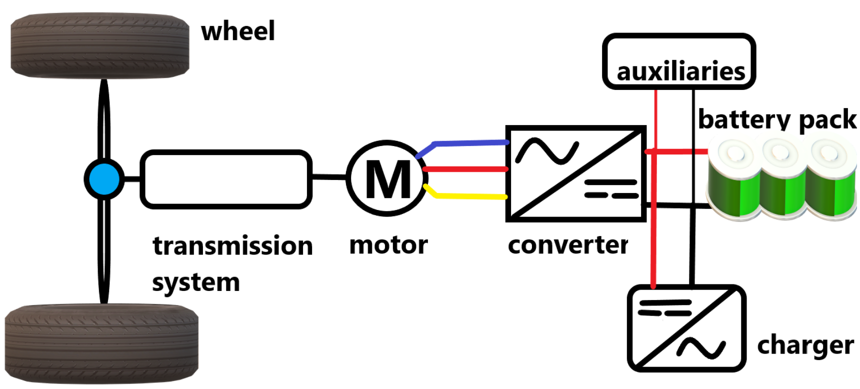

Figure 3.7: BEV powertrain

3.3.1 EV traction motors

The typical requirements of a good traction machine are high torque and power density, wide speed range, high efficiency, high reliability, less noise, and low manufacturing cost. The two widely employed traction motor types amongst EVs are IPMSM and IM. The IPMSM has appeared as the motor of choice for EV traction applications i.e. Nissan Leaf, Chevy Bolt EV, Tata Ultra Urban eBus. **Pros:** higher torque and power density, higher efficiency. **Cons:** expensive due to rare earth elements (REE) in the rotor. Unlike the IPMSM, the IM does not make use of the REE which makes the IM more attractive in terms of cost perspective. **Pros:** simple in construction, robust, reliable, versatile, and less maintenance. **Cons:** the IM has lower efficiency and torque density as compared to the IPMSM [11, 36–39]. This research only concentrates on the IPMSM as it is the most common machine amongst EVs.

3.3.2 EV traction battery pack

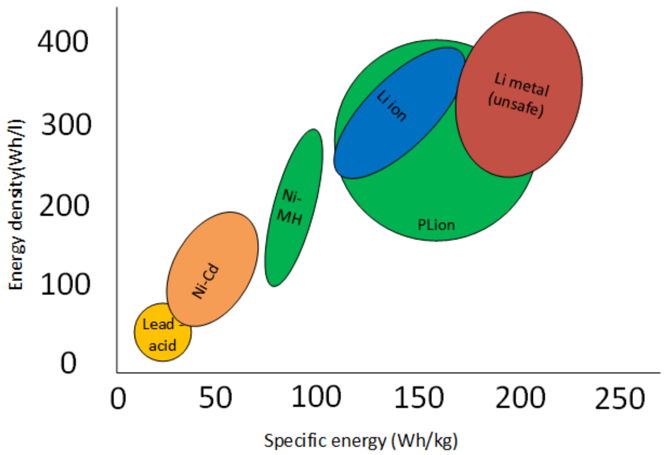

Figure 3.8: Specific energy versus energy density in battery technologies

The Lithium ion (Li ion) battery technology has emerged to be the most prevalent energy storage for EVs and consumer electronics. This is due to the fact that generally, it has a high specific energy, high specific power, high efficiency, and a long life cycle as compared to the other technologies as shown in Fig. 3.8. Fig. 3.9

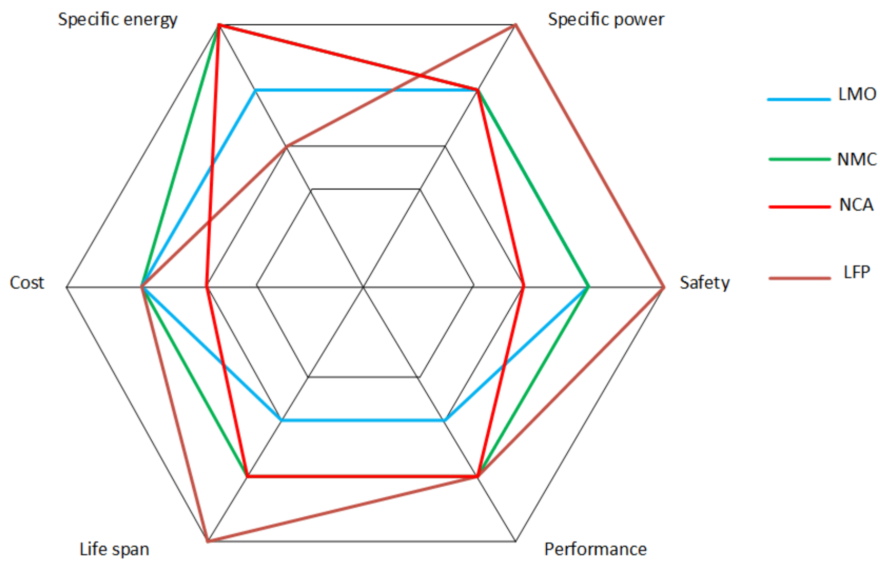

Figure 3.9: Battery hexagonal spider performance index

shows the performance index of the four Li-ion families that largely dominate the EV battery market: Lithium-Nickel-Cobalt-Aluminum (NCA), Lithium-Nickel-Manganese-Cobalt (NMC), Lithium-Manganese-Oxide (LMO) and Lithium-Iron-Phosphate (LFP). Lithium-Cobalt-Oxide (LCO) battery is mostly expended in consumer electronics but not utilized in EVs due to underlying safety concerns and costly cobalt prices. Lastly, there is also Lithium Titanate (LTO) which has an excellent C-rate but it is rarely used in EVs because it has a very low specific energy yet is expensive [4, 40–44]. ESSs are not a major concern for this research work.

3.4 EV Powertrain Configurations

The powertrain of an EV has numerous configurations such as the ones shown in Fig.3.10:

A. front-wheel drive

B. rear-wheel drive

C. both front and rear-wheel drive

D. 2-motor rear-wheels drive

E. 2-in-wheel motors front drive

F. 4-in-wheel motors drive

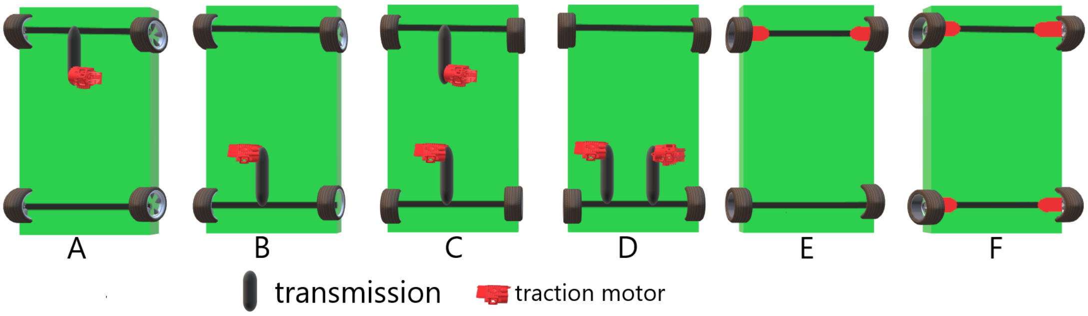

Figure 3.10: Powertrain Configurations

Each architecture has its own pros and cons with regard to safety, reliability, energy efficiency, performance, and cost. The configurations with several motors have redundancy which enhances the reliability of the system, thus safer. The multiple motors also share the required power which reduces the power ratings of each motor and converter. The in-wheel technology further improves the compactness and energy efficiency of the powertrain [18, 45]. The models in this research work only consider the 2-in-wheel motor front-drive powertrain configuration.

3.5 Summary

This chapter comprises vehicle longitudinal dynamic equations in relation to energy consumption in the traction motor. The elements that affect energy consumption in an EV which consist of the technical parameters of the EV, efficiency map, and the drive cycle were considered in this chapter. Lastly, a general setup of BEV was also looked at. This included an overview of common traction motors in EVs, battery technologies, and the different powertrain configurations in EVs.

CHAPTER 4

Electric Vehicle Modelling in Matlab/Simulink

4.1 Introduction

Model-based design approach employs Matlab/Simulink application to model an EV model. Either powertrain block sets or Simulink equations can be used to build an EV Simulink model. The latter is utilized in this chapter to implement the vehicle's longitudinal dynamic equations that were described in Chapter 3. The former usually needs a lot of other parameters which were not readily available, thus it was not preferred in this study. The EV Simulink model is then validated against a real EV that was built by eco-students from the Technical University of Munich (TUM). Firstly, EV Simulink model validation is carried out by observing if the model is able to follow and track real the drive cycle by TUM EV. This is done so as to make sure if the PID controller which acts as the driver has been set properly and also to ascertain if the EV model satisfies the drive cycle demands. Secondly, a comparison in terms of energy consumption between the Simulink EV model and TUM EV is made for the drive cycle.

4.2 EV model

The approach to enact this model is called the model-based design. It employs Simulink equations to represent the mathematical dynamics of the EV. In this way the performance aspect and energy consumption of the EV can be analyzed. The input to the Simulink EV model is a drive cycle that characterizes the time-velocity performance of the vehicle. The enlisted dynamic equations in Chapter 3 were implemented in Matlab/Simulink as shown in Figs. 4.1, 4.2 and 4.3, respectively. Fig. 4.1 shows the whole EV Simulink model.

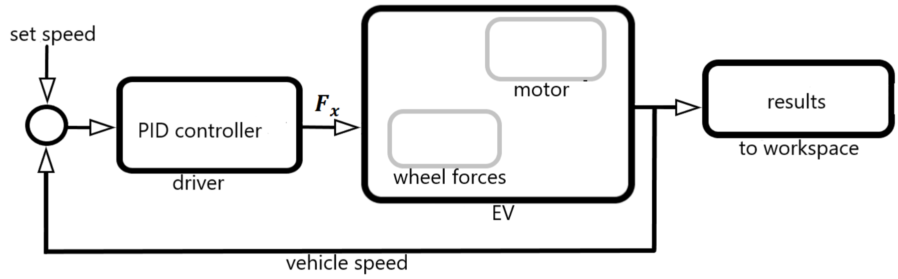

Figure 4.1: EV model and driver

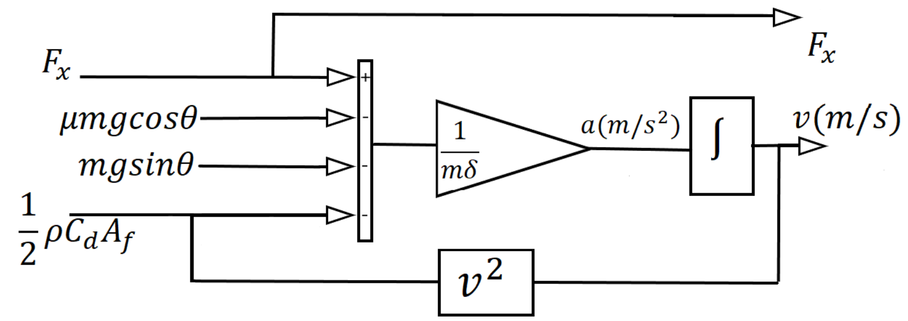

Figure 4.2: Wheel forces

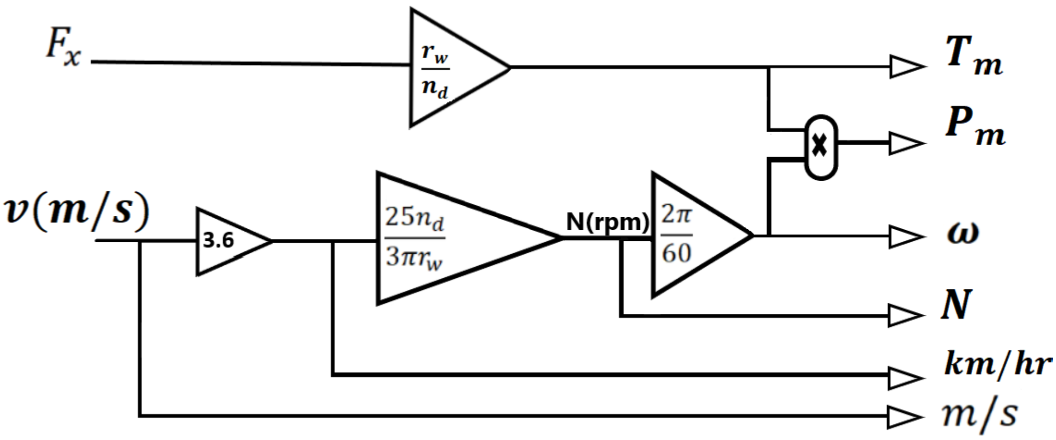

Figure 4.3: Dynamic equations block

The vehicle's velocity is sampled at the output and compared to the set velocity which is the desired vehicle's velocity. These two are then fed into a compactor which produces an error signal. A proportional integral derivative (PID) controller which acts as a driver takes the error signal and generates the required traction force, F_x, such that the vehicle speed is the same as the set speed. In that way, the EV can be made to follow the speed of any drive cycle. F_x is then given to Fig.

4.2, to execute the summation of all the forces acting on the vehicle which then resolves the acceleration of the vehicle. Acceleration is integrated to determine the longitudinal velocity of the vehicle which is also integrated in order to compute the distance covered by the EV. F_x and velocity signals are then taken to Fig. 4.3 where T_m, w, N, and km/hr are calculated. T_m and N are then used to calculate P_m per second on the shaft of the traction motor. This gives the mechanical shaft energy consumption for each operating point per second on the shaft of the motor. T_m and N are then plotted on the efficiency map of the electric traction machine. In this way, an efficiency value for each operating point is determined. This is then used to translate the mechanical shaft energy to the input electrical energy from the battery. But, during regenerative braking, the process is vice-versa. The total energy is an addition of all the energy consumption per second for the duration of the drive cycle.

4.2.1 Simulink model

Fig. 4.4 shows the overall setup of the Simulink EV model. Fig. 4.5 shows how the PID driver process the tractive force required for propulsion by comparing the vehicle speed to the reference speed. Fig. 4.6 shows how the vehicle dynamics are calculated by using the tractive force from the PID controller. All the calculations in the output results were done per second.

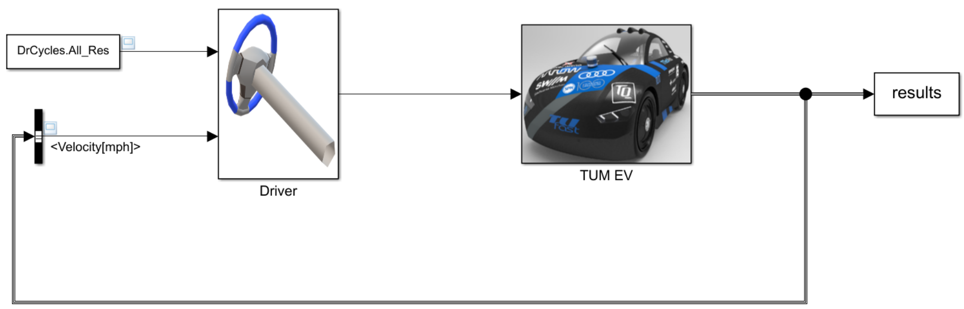

Figure 4.4: TUM EV in Simulink

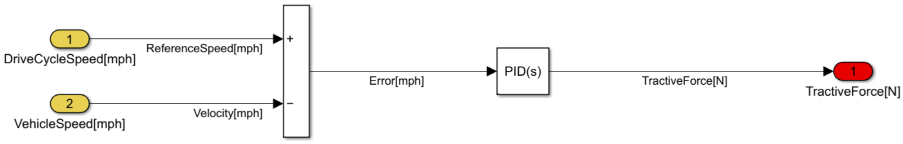

Figure 4.5: TUM EV driver in Simulink

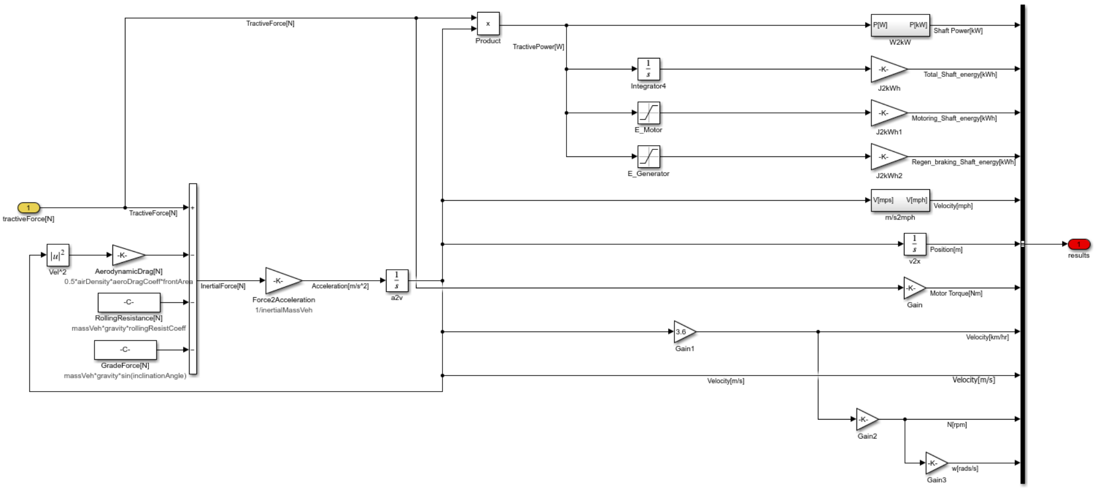

Figure 4.6: TUM EV dynamics in Simulink

4.3 Technical University of Munich Electric Vehicle (TUM EV)

An actual racing EV shown in Fig. 4.7 that was built from scratch by TUM eco-students for their 2019 Shell Marathon Competition will be used to validate the Simulink EV model. Table shows the technical parameters of the TUM EV. Fig. 4.8 shows the energy flow from the battery to the motors in the TUM EV. The electrical power is provided by a 13-cell Lithium polymer battery, which is monitored by a battery management system (BMS).

Figure 4.7: Technical University of Munich electric vehicle

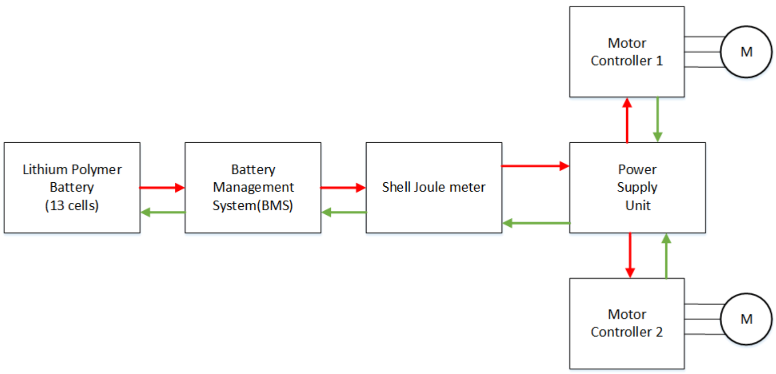

Figure 4.8: The energy flow diagram in the EV

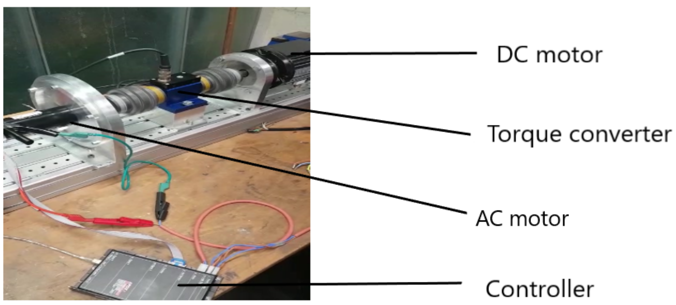

Figure 4.9: Laboratory motor testing set up

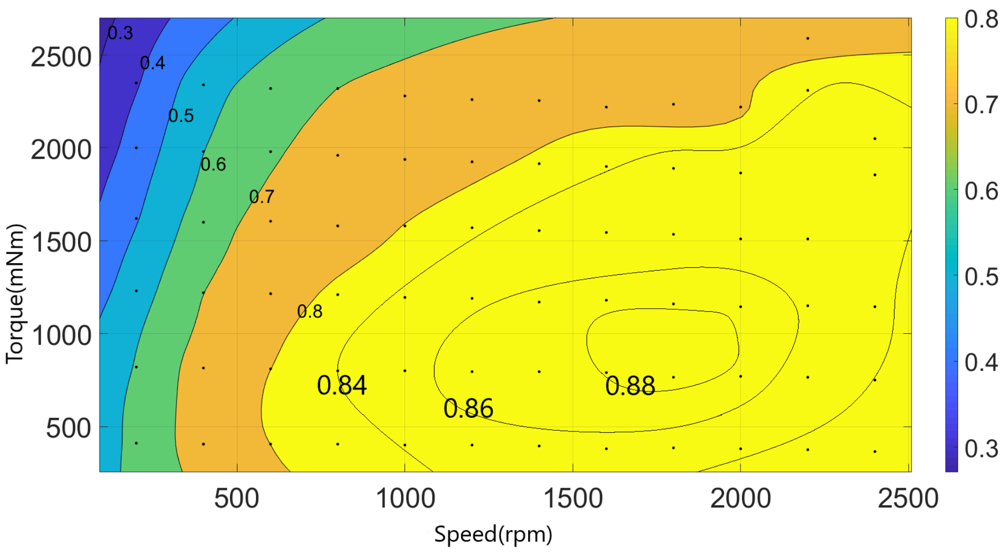

Figure 4.10: Efficiency map of each motor on the electric vehicle

Table 4.1: TUM EV technical parameters

$m = 173\ [kg]$	$\rho = 1.225\ [kg/m^3]$	$\delta = 1$	$\theta = 0\ [rad]$
$A_f = 1\ [m^2]$	r_w=0.279 [m]	$n_d = 7.105$	$\mu = 0.0035$
$C_d = 0.3$	$g = 9.81\ [m/s^2]$		

Table 4.2: TQ ILM85X13 IPMSM specification [1]

specification	value
maximum power (w)	440
nominal voltage (v)	48
nominal current (A)	10.8
terminal resistance (Ω)	0.22
maximum efficiency (%)	92
rated torque (N·m)	1.44
Torque constant (mN·m/A)	134
Peak Torque (N·m)	4.66
rpm speed	2950
outer stator diameter (mm)	85
stator length (mm)	27.2
inner rotor diameter (mm)	52
rotor length (mm)	15.7
mass (g)	400
number of pole pairs	10
Rotor inertia I ($kgcm^2$)	0.61

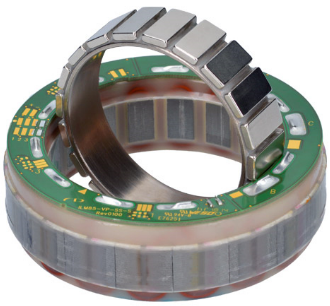

Figure 4.11: TQILM 85x13 motor [1]

During motoring (red arrow), power flows from the battery through the BMS, which includes emergency switches and a relay for power cut-off. An emergency stop can be initiated by the BMS in case of a malfunction in the battery. Consumption measurement for the whole vehicle except the horn is done by the joule meter between the BMS and the power supply unit (PSU). After passing the PSU

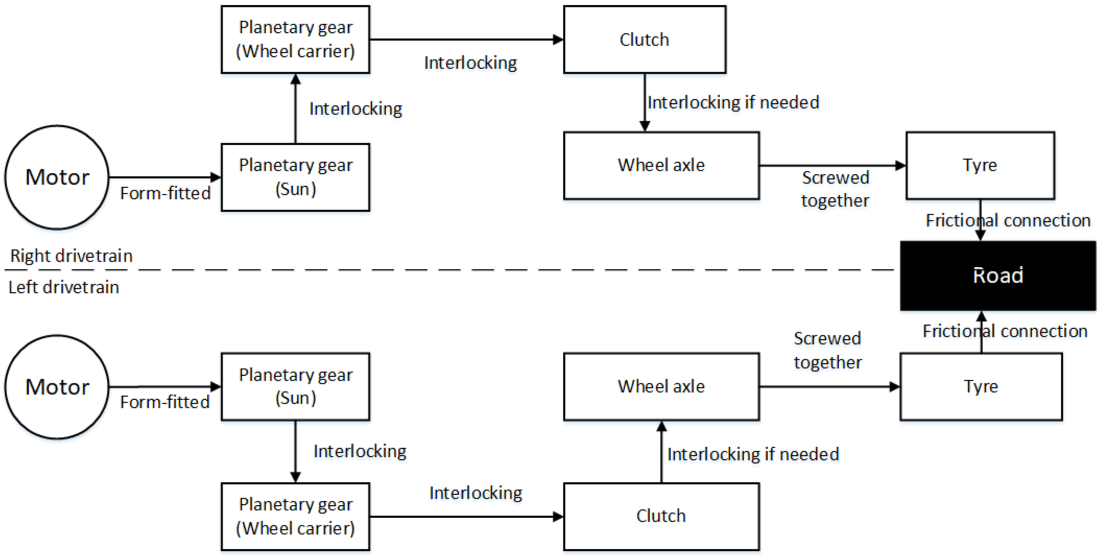

Figure 4.12: Propulsion system

and the motor controllers, electric power then flows into each of the two in-wheel propelling IPMSMs (TQ ILM 85x13). The specifications of this frameless motor are shown in Table 4.2 and Fig. 4.11 shows its rotor and stator setup. During regenerative braking(green arrows), electric power flows in the opposite direction all the way to the battery where it is stored. The TQ ILM 85X13 electric motor was first separately driven on a test bench in the experimental setup as shown in Fig. 4.9 where the following parameters were measured: input current plus voltage and the output speed(rpm) and torque(N·m) on the shaft. These measurements were done in steps of 200rpm up until 2400rpm whilst the torque was measured in steps of 0.41N·m until 2.4N·m. The efficiency values of each operating point were calculated after which the data was exported into Matlab where it was used to map out the efficiency of the motor operating points as shown in Fig 4.10. Interpolation was used to cater to the motor speeds and torque points which were not measured. The propulsion system of this EV consists of two symmetrical drivetrains, one on the left and one on the right as shown Fig. 4.12. The motor converts the electrical energy and produces a mechanical torque which drives a planetary gear that is coupled to the wheel carrier. The wheel carrier is coupled to the wheel axle through a clutch. If the clutch is engaged force is transmitted to the wheel axle and tire which interacts with the road through frictional force and thus, thrust the vehicle into motion. All the drive-line and the propulsion system components are designed for optimal efficiency which helps to elongate the mileage coverage of the EV.

4.4 Simulink EV Model Validation

TUM EV was test-driven on a test track and its velocity-time profile (drive cycle) was measured. This drive cycle was then simulated in the Simulink EV model. The performance between the two was compared in terms of how the PID controller is able to track the real drive cycle and energy consumption on the test track. Fig. 4.13 shows a comparison between the drive cycle of the TUM EV (red) and the Simulink EV model (blue).

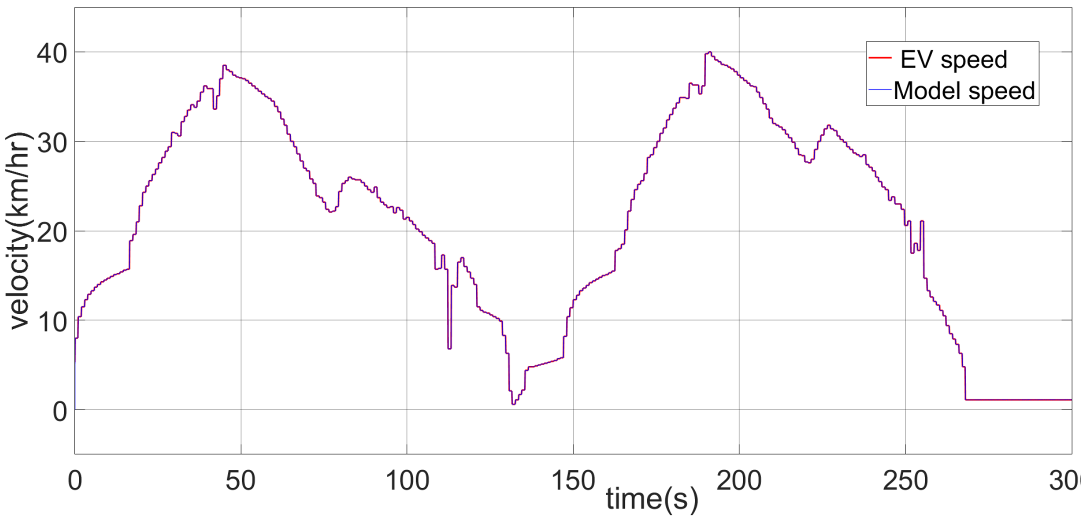

Figure 4.13: Validation test drive

The PID controller which acts as the driver is able to track and follow the real drive cycle. This is an important step since it ascertains that the EV model is capable of satisfying the drive cycle demands and that the PID was tuned correctly. Fig 4.14 shows test drive energy consumption of the TUM EV (red) and the Simulink EV model (blue). An error between the EV and model was found to be 1.8% and this error seemed to be more noticeable at higher velocities. This error could be attributed to an increase in aerodynamic drag force due to an eventual headwind velocity. The EV model neglects the headwind velocity. The interpolation of

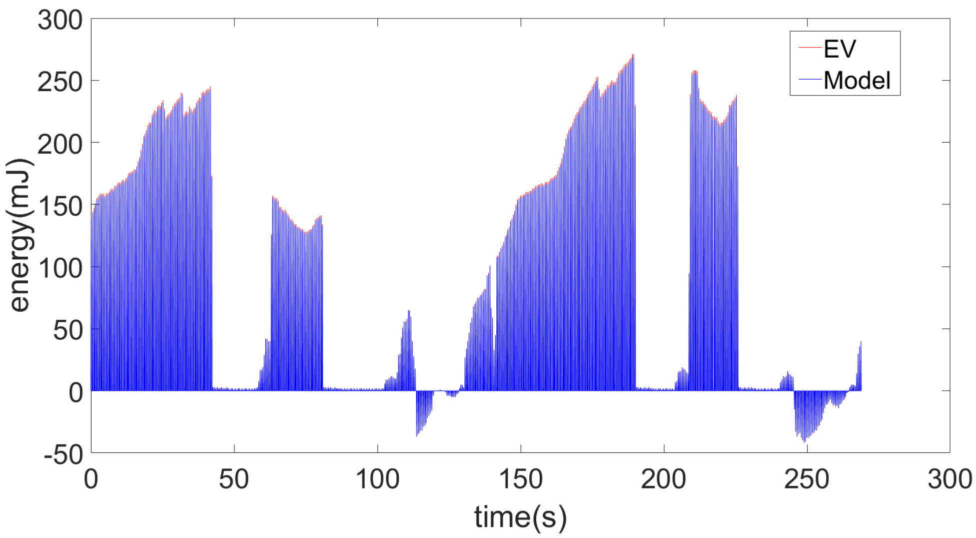

Figure 4.14: Validation test drive energy consumption

the efficiency map and the fact that the model is unable to account for energy consumption due to auxiliaries i.e power steering, light, and the horn could also contribute to the error.

4.5 Summary

An EV model was developed in Matlab/Simulink environment by considering the vehicle dynamic equations. The model was then validated by a drive cycle from a real EV. It is realized that the PID controller driver is able to trace the real EV drive cycle. The Simulink EV model and TUM EV closely match each other in terms of energy consumption. But a slight error of 1.8% between the two is attributed to the aerodynamic drag coefficient and to the inaccuracies of the efficiency map due to interpolation.

CHAPTER 5

Eco-driving Strategy

5.1 Introduction

Eco-driving is an active area of research that appears to contribute immensely towards a solution to mileage anxiety amongst EV drivers, as it makes the EV optimally utilize the onboard finite energy storage. Such a driving technique is vital to sustaining the EV on the road considering the fact that charging stations density is still very low in most parts of the world. Moreover, even if the charging stations are available, the current technology of batteries is still very much limited in terms of battery C-rate. Eco-driving looks at how the vehicle dynamics together with the vehicle technical parameters, the traction motor efficiency and the road gradient can be employed to formulate a driving style that can favour the usage of optimal energy during a drive cycle. The eco-driving strategy entails both optimal speed driving and energy-efficient acceleration. This chapter is concerned with the design and development of an eco-driving strategy for EVs. Hence, this chapter separately contributes to the implementation of an optimal speed algorithm and energy-efficient acceleration algorithm through the usage of an EV Simulink model. The eco-driving strategy is then validated so as to realize its benefits by test driving the TUM EV which is used as a prototype in this research. This chapter also contributes to the study and development of the different acceleration and deceleration modes beyond the optimal speed.

An eco-driving study is an important step, both before the purchase and during the EV operation. In the process before the procurement of the EV, it helps the end-user to be able to choose an EV with technical parameters which are oriented towards good overall energy efficiency for a particular drive application (drive range with a known grade). It is during this stage that the user can be able to choose an EV with the most efficient aerodynamic coefficient C_d, a smaller frontal area A_f and tyres with an excellent kinetic coefficient of friction μ. The gross EV mass is also considered here because it singly determines the force of inertia and the climbing force. These two forces consume a lot of energy, especially in a city drive that is characterised by a lot of hilly drive ranges with a lot of stops. The type of traction motor and the shape of its efficiency contours can be chosen here since the motor is the component of the EV that consumes most of the energy from the battery. Finally, during the operation of the EV, eco-driving necessitates the determinant of an optimal speed for a certain drive range. And then it looks at how the EV can be accelerated to achieve the optimal speed efficiently.

5.2 Optimal Speed Driving Strategy

The optimal speed algorithm attempts to establish a speed at which the vehicle consumes the least amount of energy (kWh) from the battery during a driving schedule. As it has already been stated, the energy consumption of the EV depends on mass, rotational mass coefficient, acceleration, kinetic coefficient of friction, road gradient, aerodynamic drag coefficient, frontal area, velocity, transmission system efficiency, wheel radius, gear ratio, motor efficiency, time and battery efficiency (superimposed with converter efficiency). But once the EV has been manufactured and delivered to the end-user, energy consumption significantly depends on acceleration, velocity, time, road gradient, battery efficiency, transmission system efficiency and motor efficiency. Transmission and battery efficiencies are assumed to be constant in this study. Optimal speed driving strategy is mainly dependent on constant speed driving. It ignores vehicle acceleration since it will be covered separately in its own section. During a constant velocity, acceleration is zero, thus the traction force F_x, on the wheels becomes:

$$F_x = \mu mgcos\theta + mgsin\theta + \frac{1}{2}\rho C_d A_f (v + v_0)^2 \qquad (5.1)$$

therefore, the motor is only needed to provide a steady-state torque T_{ss}, calculated as:

$$\begin{aligned} T_{ss} &= \left(\frac{F_x}{\eta_T}\right)\left(\frac{r_w}{n_d}\right) \\ &= \frac{\mu mgcos\theta + mgsin\theta + \frac{1}{2}\rho C_d A_f (v+v_0)^2}{\eta_T}\left(\frac{r_w}{n_d}\right) \end{aligned} \tag{5.2}$$

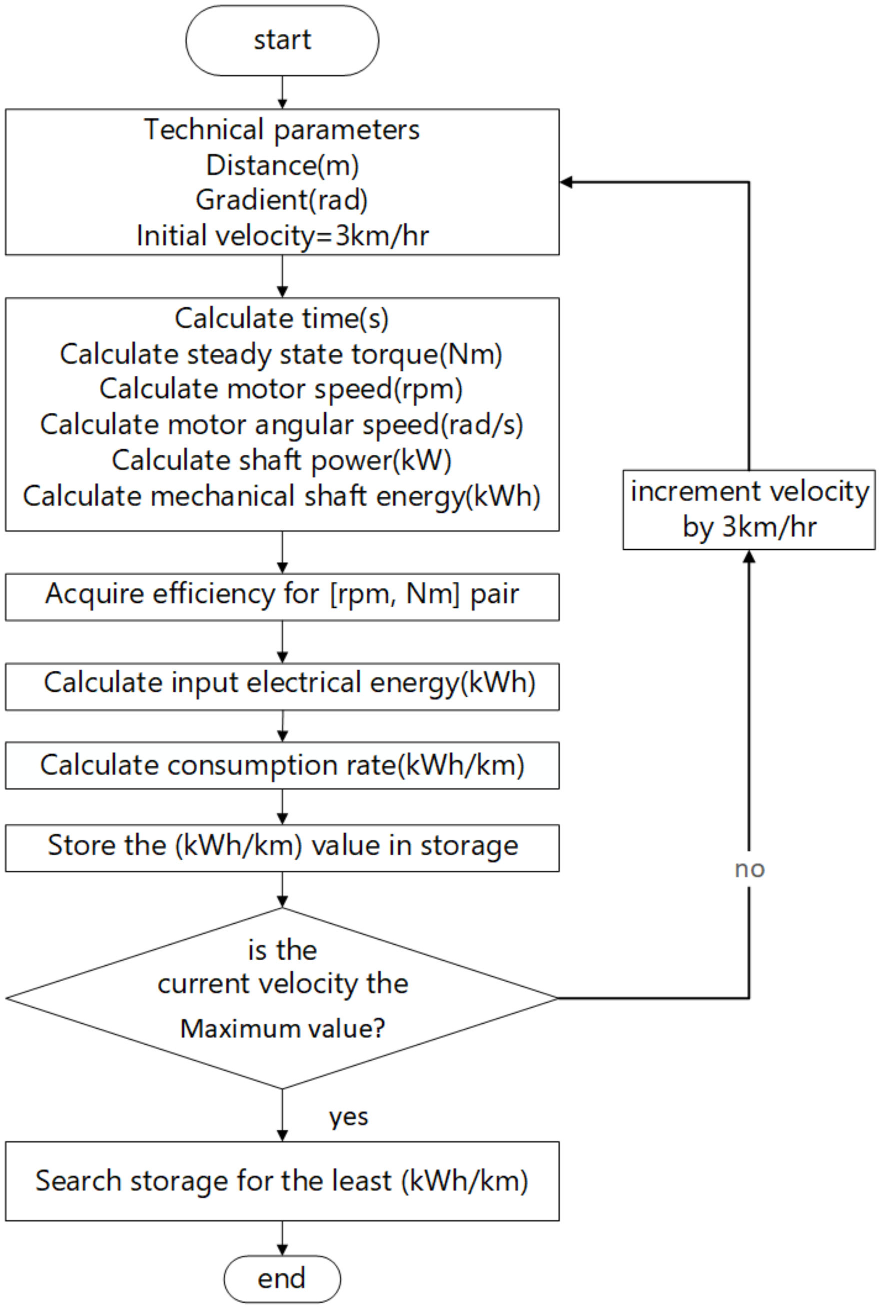

Figure 5.1: Optimum speed algorithm

T_{ss} is the torque that the motor is required to provide in order to keep the EV at a constant velocity. Assuming that the EV can be driven at any arbitrary constant velocity during or on most parts of the driving range. Hence, on this basis, an optimal speed driving strategy for TUM EV is developed by using the elevation profile of the driving range, the technical parameters in Table 4.1 and the efficiency map of the traction machine in Fig. 4.10 from Chapter 4. Fig. 5.1 illustrates the optimal speed driving algorithm in details. This algorithm follows the one in [2], except that in this work the motor torque and speed values are computed whilst the average road gradients are acquired with the assistance of Google Earth.

Primarily, the drive route (trip) is first portioned into different drive ranges according to their respective slope percentages as depicted in Fig. 6.4 in Chapter 6. A cruise speed is assumed at which that particular drive range could be traversed and then T_{ss}, motor speed and mechanical shaft energy are computed. The computed torque and motor speed pair are then used to obtain the motor efficiency from the motor efficiency map. From the obtained motor efficiency the electrical input power from the battery can be computed. The consumption of energy is then divided by the drive range distance (km) in order to determine the standard consumption rate (kWh/km) for that particular drive range at the selected cruise speed. The speed is then incremented in small steps of 3km/hr up to the velocity of 36km/hr, although this EV vehicle has a maximum of 40km/hr. The increment is conducted in this manner so that almost all the characteristics behaviour of the efficiency contours are captured in the process. Finally, the lowest consumption rate is used to determine the optimal speed for that particular drive range. This is applied for all the different drive ranges of the drive route until the end of the trip. This method is illustrated in Fig. 5.1.

5.2.1 Validation of EV Optimal Speed Driving Strategy

The optimal speed driving strategy developed in section 5.2 was first simulated using the Simulink EV model. A simulation is done at each constant speed for a 60m drive range with a zero gradient. Fig. 5.2 shows the graph of speed versus consumption rate and efficiency for this simulation. It can be noticed that the optimal speed is 24km/hr with a consumption rate of 0.138Wh/km and this occurs at an efficiency of 88%. Thereafter, the consumption rate goes up because the aerodynamic force begins to significantly increase whilst the efficiency decreases. TUM EV is then autonomously test driven on a straight flat test strip inside a hall so that the influence of ambient headwind velocity could be eliminated. The EV was accelerated to cruise velocities similar to simulations and results were recorded during constant speed. The two consumption rate graphs were plotted as shown in Fig. 5.3.

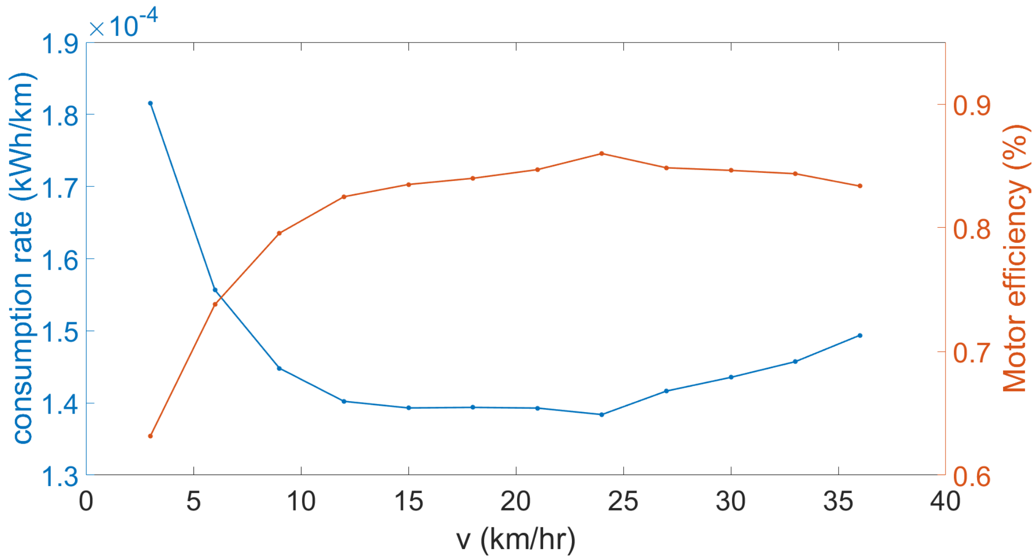

Figure 5.2: Simulink EV energy consumption rate versus efficiency(%)

The analysis of the two graphs reveals that there is an error of about 1.93% between the TUM EV and the Simulink EV model. The analysis also reveals that when TUM EV is driven at an optimal speed of 24km/hr, it is able to save 31.2% as compared to the lowest speed of 3km/hr and 8% as compared to the highest speed of 36km/hr. This is because the efficiency map is characterised by extremely poor efficiency ($\leq$ 30%) at high torque and lower speeds as depicted in Fig.4.10 in Chapter 4. But at higher speeds, the high consumption rate is due to the exponential increment in the aerodynamic force since it is directly proportional to v^2.

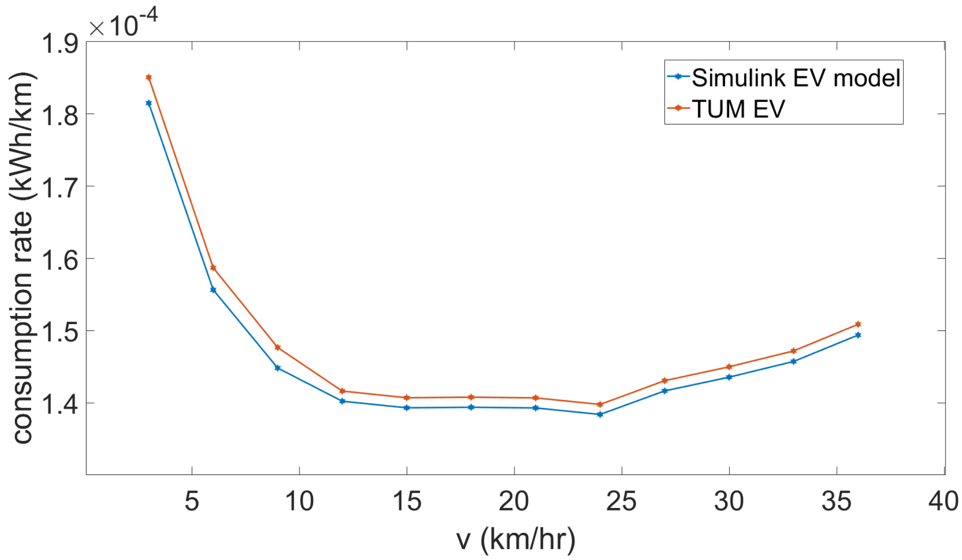

Figure 5.3: Consumption rates of TUM EV vs Simulink EV model

5.3 An Energy-efficient Acceleration Strategy

A vehicle acceleration can be achieved in different modes, either at a fast mechanism rate or at a constant rate or a slow mechanism rate. Equation (5.3) describes how the acceleration parameter β, can generate the different acceleration modes mathematically [2]. The characteristic curves are either a convex ($\beta < 1$) or a straight line ($\beta = 1$) or a concave ($\beta > 1$) acceleration architectures as shown graphically in Fig. 5.4 for $v_f = 6.7$ m/s (24km/hr), $v_i = 0$ m/s and $t_f = 20$s.

$$v = v_i + (v_f - v_i)(\frac{t - t_0}{t_f - t_0})^\beta \tag{5.3}$$

where v_i is the initial velocity, v_f is the final velocity, t_0 is the initial time, t_f is the final time and $\beta \in (0,\infty)$.

Fig. 5.5 shows an energy-efficient acceleration strategy that is employed to determine the acceleration energy consumption rate of a vehicle. This procedure designs an algorithm to determine an acceleration mode in which the vehicle's energy consumption is minimal during the acceleration process. Chronologically, as it is illustrated in Fig. 5.5, equation (5.3) is integrated to calculate the distance

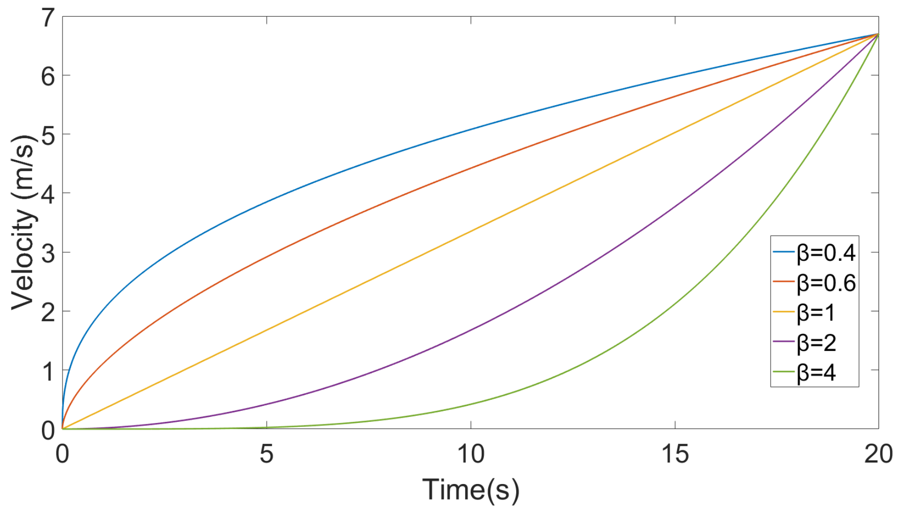

Figure 5.4: Various acceleration modes

covered during acceleration. Then, equation (5.3) is differentiated to calculate acceleration. The motor speed, torque, power and mechanical shaft energy are then calculated. The efficiency value for torque and motor speed pair is acquired on the efficiency map after which its used to calculate the battery energy consumption. Thus, the energy consumption rate (kWh/km) can be calculated for each operating point. A drive range with a zero-road gradient ($\theta = 0°$) is used for all acceleration energy consumption rate calculations in this research. This is done in order to avoid the biases of the road gradient on the efficiency map. But otherwise, the energy-efficient strategy can work for any road gradient.

5.3.1 Validation of energy-efficient acceleration strategy

The energy-efficient acceleration strategy was simulated with the Simulink EV model according to the algorithm in Fig. 5.5 for the curves $\beta = 0.4$ and $\beta = 4$ as shown in Fig. 5.4. $\beta = 0.4$ and $\beta = 4$ acceleration modes, were chosen because they were the modes with the minimum and maximum energy consumption possible for TUM EV, respectively. TUM EV was then experimentally test-driven to accelerate according to these styles as shown in Fig. 5.6. These accelerations were achieved through autonomous driving since it is nearly unpractical for a human driver to perfectly achieve such characteristic curves. This is done in order to clearly show

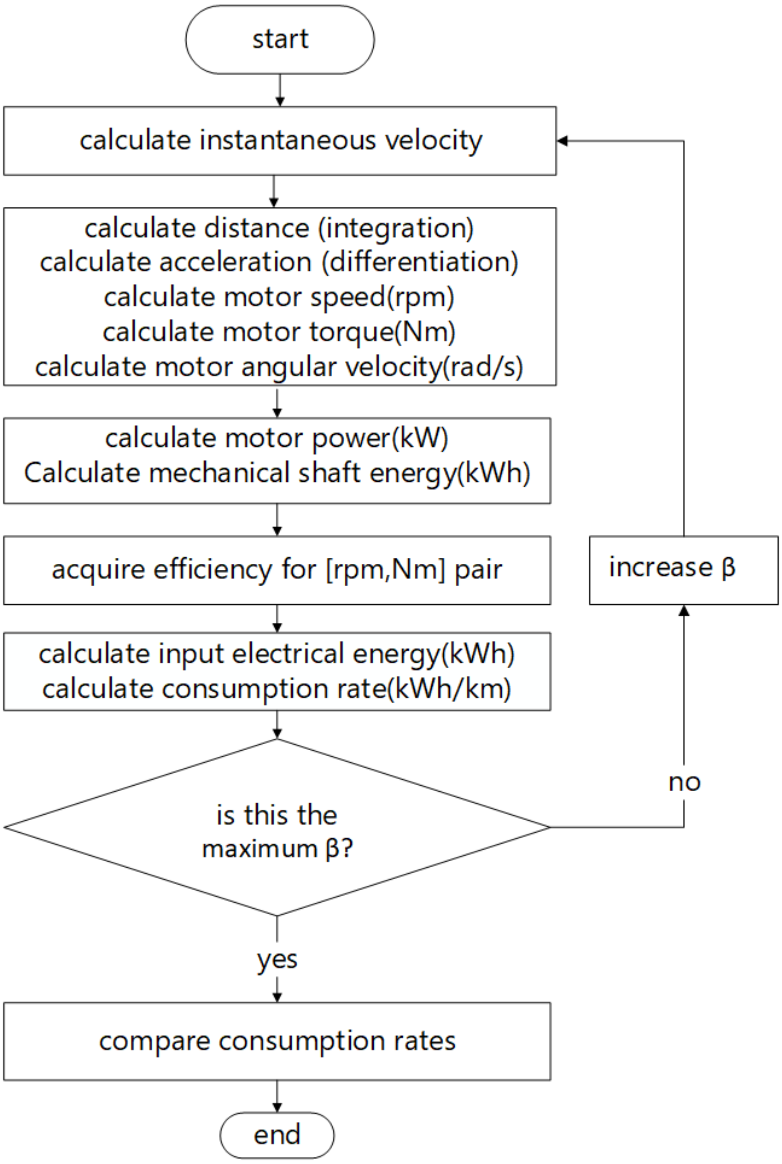

Figure 5.5: Optimum acceleration algorithm

the energy consumption behaviour between an acceleration of $\beta < 1$ and $\beta > 1$ without any ambiguity.

Table 5.1: Simulation versus real energy-efficient acceleration

parameter	simulation(Wh)	gain(%)	experiment(Wh)	gain(%)
$\beta = 0.4$	2.06	-	2.10	-
$\beta = 4$	2.79	35.43	2.80	33.33

Table 5.1 compares the energy consumption for simulation and experimental results for a convex ($\beta = 0.4$) versus a concave ($\beta = 4$) acceleration modes. It can be seen from both sets of results in this table that the convex mode is efficient

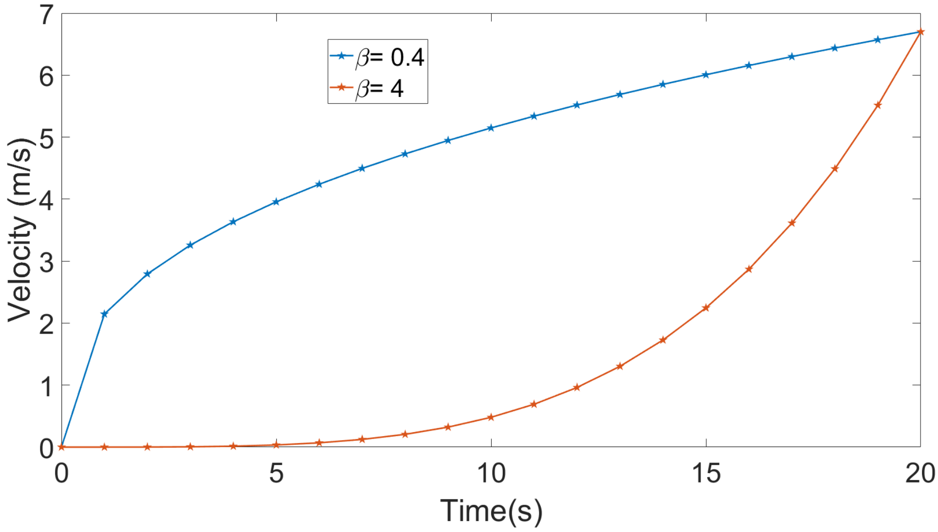

Figure 5.6: TUM EV acceleration test

and that the concave is inefficient. The convex acceleration architecture is generally referred to as the "as-fast-as-possible" acceleration mode because the vehicle reaches high velocities quickly. While the concave acceleration style is referred to as the "as-slow-as-possible" acceleration architecture since the vehicle takes a while to acquire high velocities. The simulation results show an energy saving of 35.43% whilst the experimental results show a saving of 33.33% between the two acceleration architectures. It can be noticed that the lesser the acceleration parameter, the lesser the energy consumption. This is because the IPMSM efficiency map has a poor efficiency region at high torque and lower speeds as already shown in Fig. 4.10. Thus the quicker the EV can be accelerated to the optimal speed which is located at an efficient region, the overall energy consumption can be reduced. However, during regenerative braking from the optimal speed towards zero (standstill), deceleration should be done as slow as possible.

5.3.2 Other Energy-efficient Acceleration Modes

So far acceleration energy consumption rates have been investigated from zero speed (standstill) or lower speed to the optimal speed of 6.7 m/s (24km/hr). As already stated, the as-fast-as-possible acceleration mode was found to be the uttermost efficient in this region. Arrow A in Fig. 5.13 exhibits this type of acceleration.

But sometimes it can happen that the driver so wishes to catch up on time since there is a minimum time on which the lap can be completed as stipulated by the competition rules. Thus, there is a need to drive the vehicle at a higher speed than the optimal speed sometimes. But this should only be done for a very short time since driving at high speeds results in higher energy consumption. This subsection explores how this could be achieved as efficiently as possible. It can be observed in Figs. 4.10 and 5.13that generally, the contours have poor efficiency $\leq 30\%$ at lower speeds. Then efficiency is in an incremental trend up to 88% which is the efficient region after which it decreases downwards. It is therefore important to investigate which acceleration mode is efficient after the optimal speed since the efficiency contours are now in a downward trend.

i. **Acceleration from optimal speed towards maximum speed**

Fig 5.7 shows TUM EV different acceleration styles for v_i=6.7m/s (24km/hr), v_f=10m/s (36km/hr) and t_f=6s and Fig. 5.8 shows its respective acceleration consumption rates.

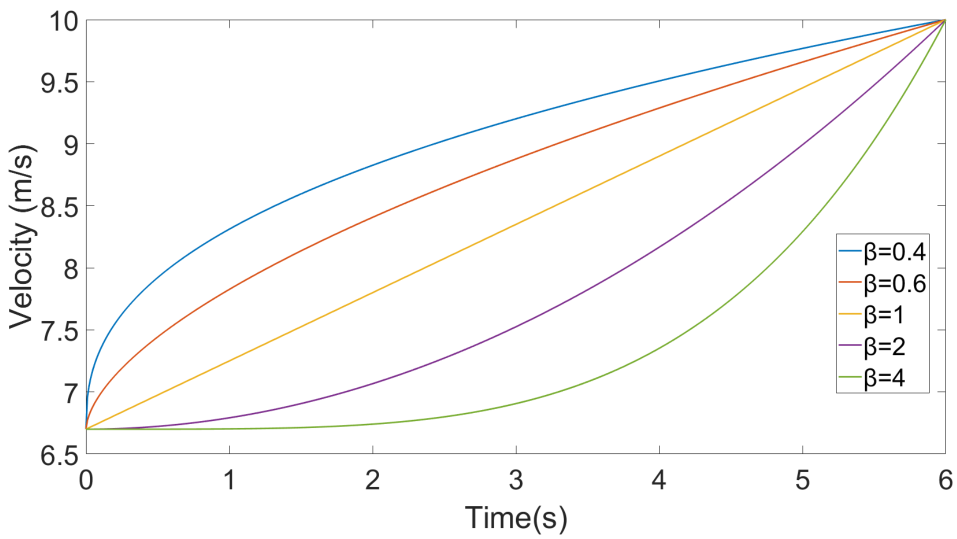

Figure 5.7: Acceleration characteristics from 6.7 m/s to 10m/s

As shown in Fig. 5.8, the β=0.4 acceleration architecture is now the most inefficient acceleration mode whilst β=4 is now the most efficient. This is because the efficiency contour values begin to decline immediately after the optimal speed of 24km/hr (17000rpm) as shown in Fig. 5.13. The β=0.4 acceleration architecture

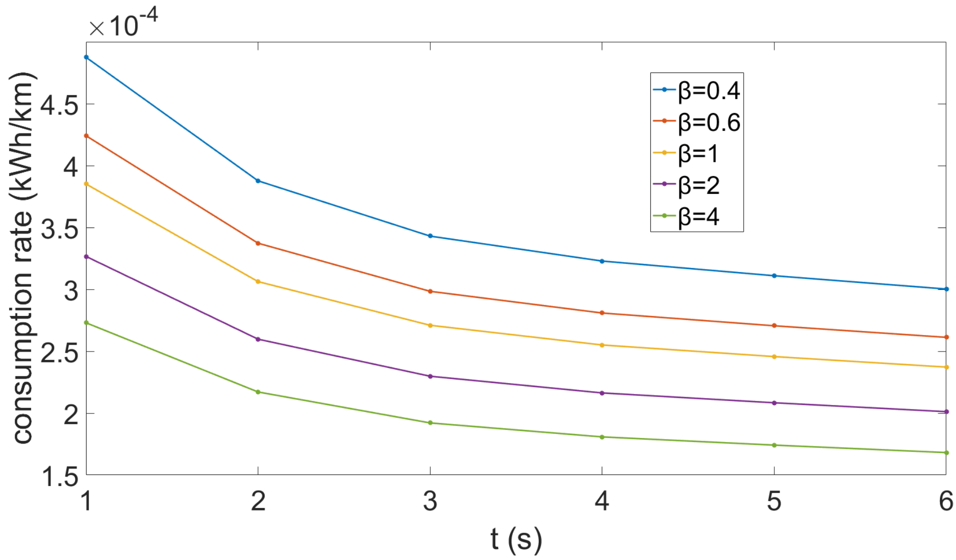

Figure 5.8: Consumption rates from 6.7 m/s to 10m/s

is inefficient because the EV accelerated faster to reach higher velocities which fall onto the inefficient region, thus most of the motor operating points will have lower efficiency values. With β=4, results in the EV remaining in the more efficient region for a longer period as it is the slowest acceleration architecture. On this grounds, the as-slow-as-possible acceleration architecture is the most efficient mode of acceleration in this region. This is depicted by arrow B in Fig. 5.13.

ii. **Deceleration from maximum speed towards optimal speed**

Fig. 5.9 shows the different deceleration from 36km/hr back to 24km/hr for v_i=10m/s (36km/hr), v_f=6.7m/s (24km/hr) and t_f=6s and Fig. 5.10 shows its energy regeneration rate respectively. It is clear that β=0.4 makes the EV recuperate more energy. This is simply because the EV quickly decelerates into the most efficient contours whereas else with β=4, the EV remains on the least efficient contours for a longer time. Hence, the fast-as-possible acceleration architecture regenerates more energy from the wheels as compared to the other deceleration modes. This is represented by arrow C in Fig. 5.13.

iii. **Deceleration from optimal speed towards zero speed**

Fig. 5.11 shows the possible different deceleration modes from 24km/hr back to zero. This is for for v_i=6.7m/s (24km/hr), v_f=0m/s and t_f=6s and Fig. 5.12

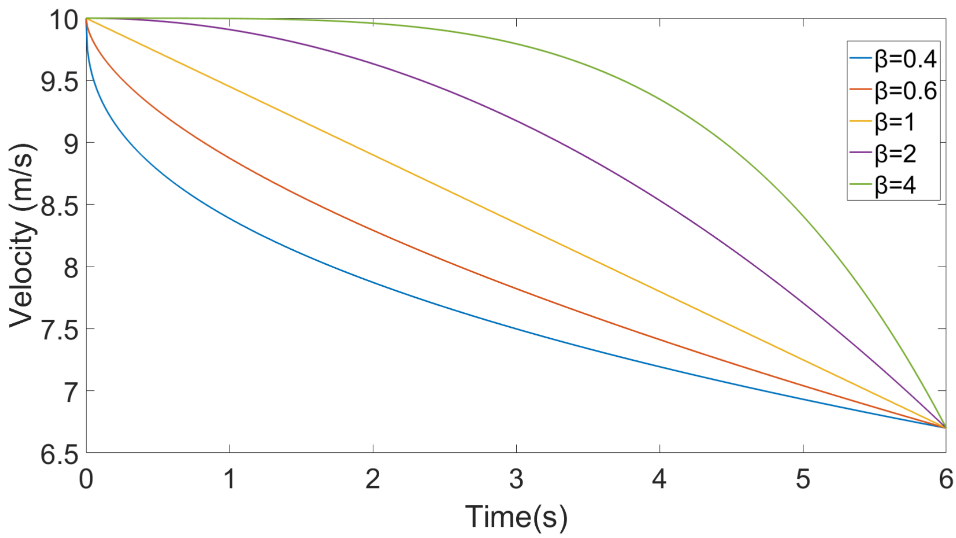

Figure 5.9: Deceleration characteristics from 10m/s to 6.7m/s

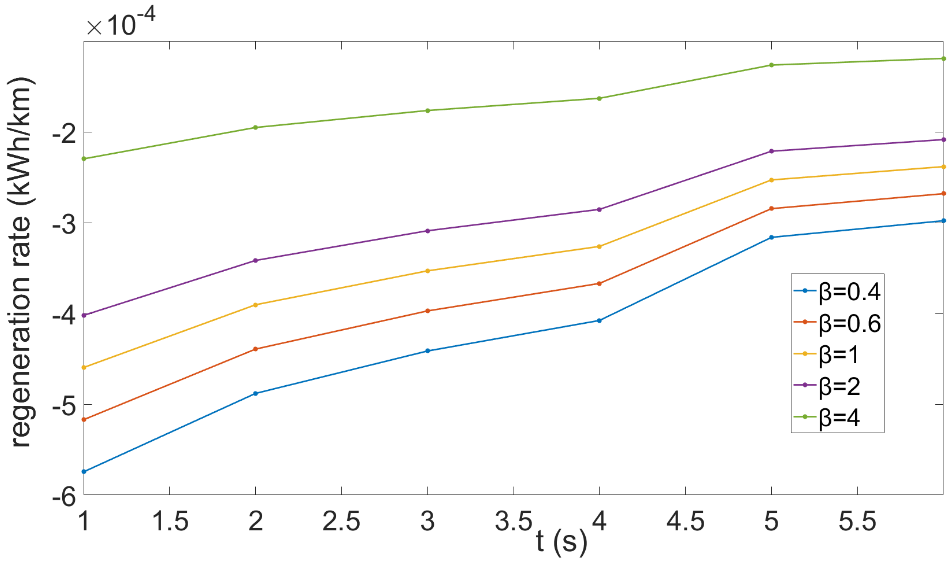

Figure 5.10: Deceleration regeneration from 10m/s to 6.7m/s

shows the energy regeneration rate respectively. The $\beta = 4$ mode makes the EV recuperate more energy since it results in the EV remaining in the more efficient region much longer as compared to the rest. And so the as-slow-as-possible mode is the most suitable deceleration mode in this region. Arrow D represent this deceleration style in Fig. 5.13.

Four energy-efficient acceleration architectures

Fig. 5.13 shows the four energy-efficient acceleration/deceleration modes. These are largely dictated by the shape of the efficiency map in relation to the location

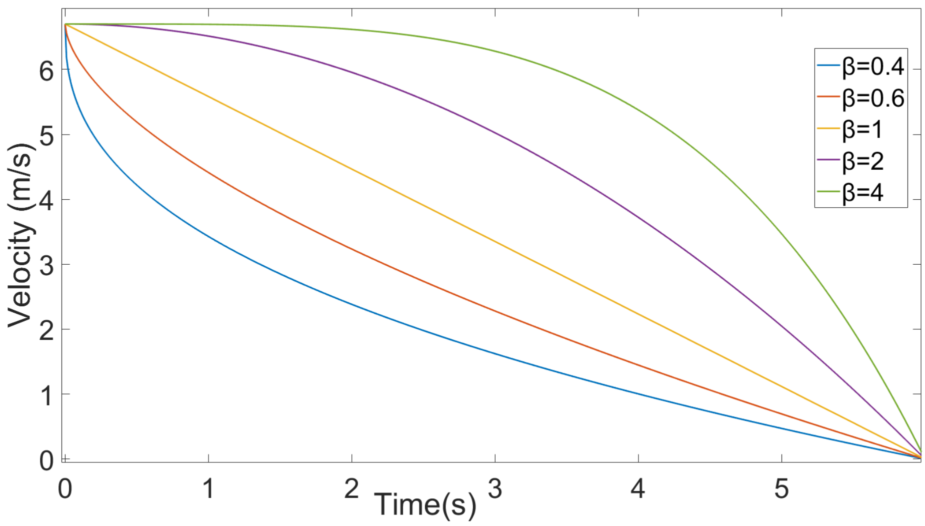

Figure 5.11: Deceleration characteristics from 6.7m/s to 0m/s

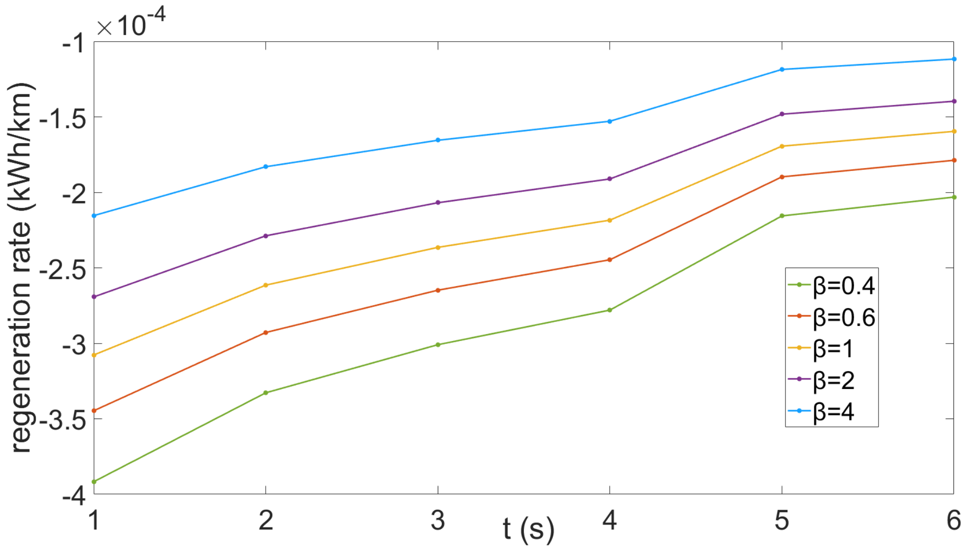

Figure 5.12: Deceleration regeneration from 6.7m/s to 0m/s

of the most efficient region of the efficiency map. This is the reason why the shape of efficiency contours on the efficiency map plays a very crucial role. Firstly, the shape of the efficiency contours determines where the optimal speed lies. Secondly, it also decides on the type of the acceleration mode which is suitable for the region.

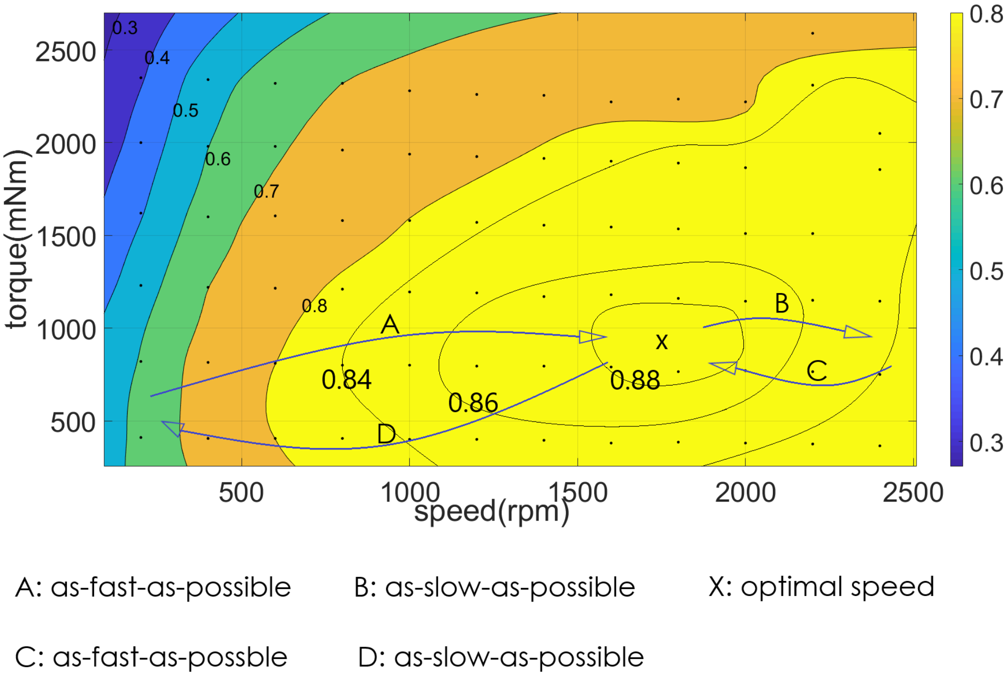

Figure 5.13: General energy-efficient acceleration architectures

5.4 Summary

The purpose of this chapter was to separately design, develop, implement and validate the elements of an EV eco-driving strategy. In both strategies, this entails the computational procedure of both the motor torque and motor speed and then calculating the battery energy consumption by using the motor efficiency map. TUM EV was then test-driven according to the eco-driving algorithm in a bid to realise the benefits in terms of energy consumption from the battery storage. TUM EV was found to have an optimal speed of 24km/hr and savings of up 8% and 31.2% between the optimal speed and the highest speed and lowest speed were realized, respectively. This is because during lower speeds the efficiency is very poor whilst at higher speeds the energy consumption rate is largely dominated by the spike in the aerodynamic force due to the rise in velocity. The reason why the consumption is minimal at 24km/hr is that it lies in the most efficient region of 88%. It was found that the as-fast-as-possible acceleration architecture useless consumption of energy during vehicle acceleration from zero to optimal speed. There was an energy saving of up 33.33% between $\beta = 0.4$ and $\beta = 4$

acceleration modes, experimentally. Accordingly, if an EV is driven strategically, energy consumption from the battery could be minimized, since the electric motor has operating regions of high efficiency and low efficiency. The findings of this study seem to correlate with the study by the NREL in the US whereby it was found that there is a 20% energy saving on aggressively driven vehicles [20].

Other energy-efficient acceleration architectures for both acceleration and regenerative braking were also studied. It was observed that these modes were largely influenced by the shape of the efficiency contours on the efficiency map. It was found that the fast-as-possible acceleration style was more efficient during vehicle accelerations from zero to the optimal speed. Whereas, when accelerating from the optimal speed to the maximum speed, the as-slow-as-possible acceleration mode used minimal acceleration energy. During regenerative braking from maximum speed towards optimal speed, the as-fast-as-possible deceleration mode recuperated more energy. Lastly, the as-slow-as-possible deceleration mode regenerated more into the battery energy for vehicle deceleration from optimal speed to zero.

CHAPTER 6

Application of the Eco-driving Strategy on an eBus

6.1 Introduction

As much as eco-driving is extremely important for small-mass vehicles i.e sedans, its importance is more notable in large-mass vehicles i.e trucks, and buses. Such class of vehicles normally have large inertia, big frontal area A_f and poor aerodynamic drag coefficient C_d. All of these factors lead to a high increase in energy consumption rate. In this chapter, the eco-driving strategy that was established and validated in Chapter 5 is now applied to an eBus that is based on insert permanent magnet synchronous machine (IPMSM) powertrain. Only Matlab/Simulink simulation work will be conducted since there is no electric bus that can be used for validation. Inter-campus bus routes which are presently serviced by ICE buses will be used as a study case scenario. This study envisages the possibility of the ICE buses being replaced by eBuses. As already mentioned, a switch to EVs is highly anticipated in the near future. A comparison between eco-driving and convectional driving will be conducted. This is in order to investigate the effects of an eco-drive strategy on a more realistic drive route.

6.2 Electric Bus (eBus): IPMSM drivetrain

The eBus is a large-mass vehicle as it can be perceived from its technical parameters shown in Table 6.1 and the efficiency map of its traction machine as shown in

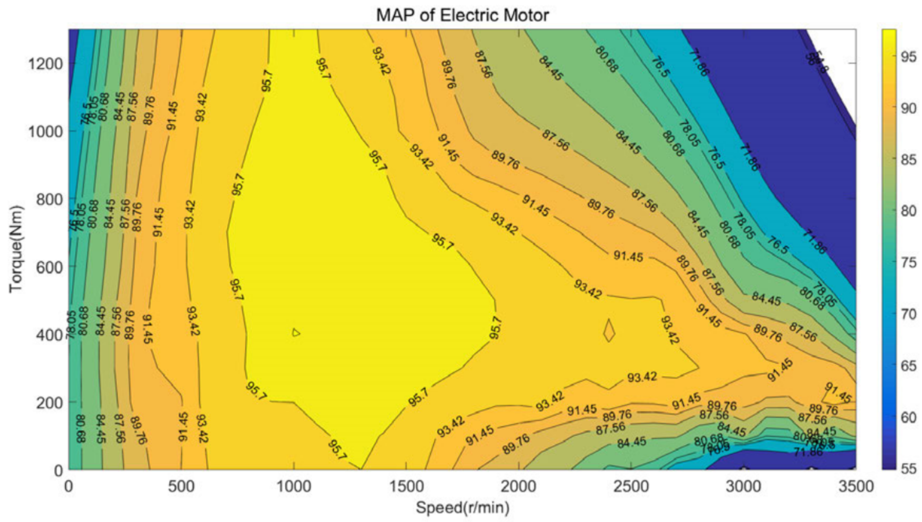

Figure 6.1: Efficiency map of the IPMSM for eBus[2]

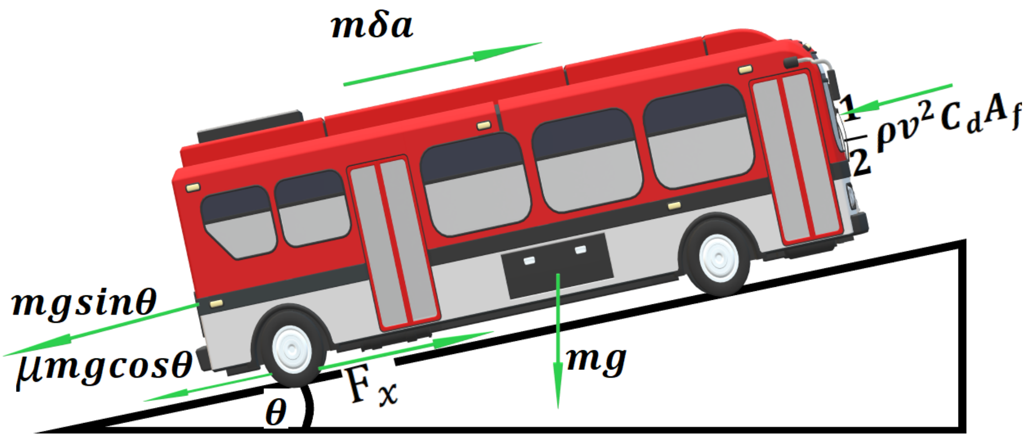

Figure 6.2: Forces that act on eBus

Fig. 6.1. As expected most of these technical parameters are large as compared to the TUM EV prototype. The IPMSM efficiency map and the technical parameters of this bus were adopted from [2]. But, the motor technology, drive-train configuration, vehicle dynamics, and motor energy consumption formulations remain the same as the one used for the TUM EV.

Table 6.1: eBus technical parameters[2]

$m = 18000\ [kg]$	$\rho = 1.225\ [kg/m^3]$	$\delta = 1.08$	$\theta = 0\ [rad]$
$A_f = 7.6\ [m^2]$	r_w=0.485 [m]	$n_d = 6.33$	$\mu = 0.012$
$C_d = 0.67$	$g = 9.81\ [m/s^2]$	$Max.\ Speed = 70km/hr$	

Currently, ICE buses drive between the campuses throughout the day as they ferry students to their respective lectures and residences. The study will be done both for a city drive (urban) and long-distance drive (extra-urban) routes as case study A and case study B, respectively.

6.3 eBus Optimal Speed Driving Strategy

A Matlab/Simulink eBus model was also developed following a similar procedure followed in Chapter 4. Fig. 6.2 shows the force diagram of the eBus. For each study case, the eBus Simulink model will be simulated to determine the optimal speed for a particular drive range of the drive route. This will be conducted by implementing the optimal speed algorithm that was developed and validated in Chapter 5. An actual speed for the ICE bus will then be measured in the driving range of interest and this will be regarded as the conventional driving strategy. An energy consumption analysis between an eco-drive and convectional driving will be accomplished in order to ascertain the benefits of eco-driving.

6.3.1 Case Study A: Urban Driving

The all-residences bus route shown in Fig. 6.3 is considered for this case study. This route was chosen because it drives via Johannesburg CBD, thus, it represents a typical city bus driving as it is often characterized by stops and go with traffic jams. It is also the busiest route, especially in the morning and it has the following bus stops: Amic Deck>>Rennie House>>Wits Junction>>Wits Education Campus (WEC)>>Ernest Oppenheimer Hall (EOH)>>Knockando>>Amic Deck. Fig. 6.4 shows the elevation profile of this route with an illustration of one of the drive ranges.

6.3.2 Case Study A: Results Analysis and Discussion

The whole drive route was first partitioned into different drive ranges according to their respective slope gradients through the help of Google Earth. Each drive range was found to have its own optimal velocity both for motoring and regeneration,

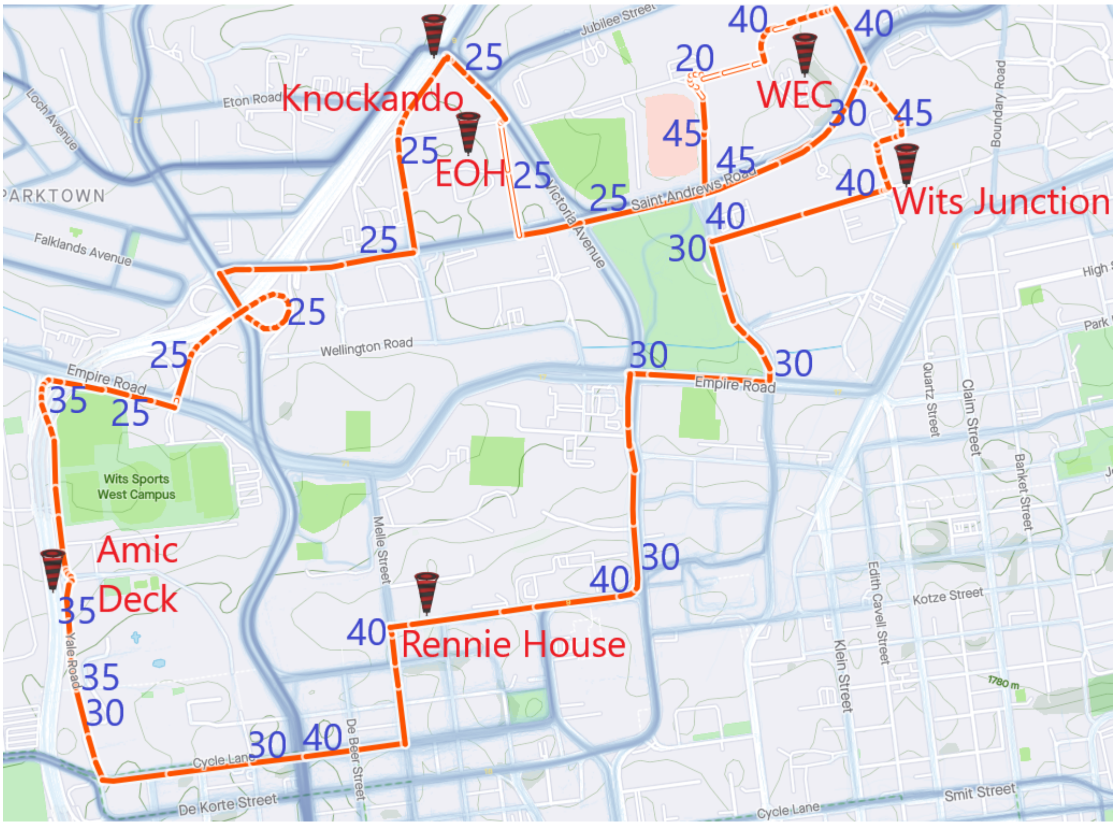

Figure 6.3: All-residences bus routes with respective optimal velocities

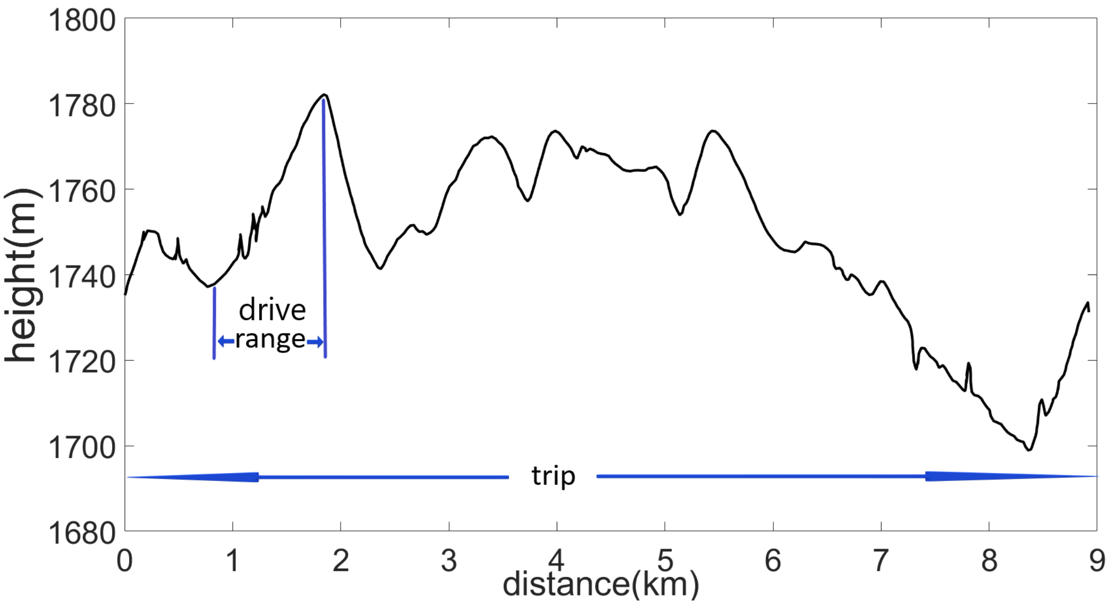

Figure 6.4: Case study A: elevation profile of the drive route

respectively as shown in Table 6.2. The optimal speeds together with their road gradients were combined into an augmented optimal speed of the eBus for the whole trip as shown in Fig. 6.5.

Table 6.2: Case study A: Drive range, gradients, optimal speed, and consumption

drive range(m)	gradient(decimal)	Opt. km/hr	kWh/km
0-262	0.064	35	2
262-773	-0.043	30	-0.7
773-1860	0.055	40	1.8
1860-2370	-0.077	30	-1.5
2370-2810	0.034	30	1.2
2810-3400	0.039	40	1.4
3400-3740	-0.047	45	-0.7
3740-3980	0.065	30	2.0
3980-4190	-0.033	45	-0.4
4190-4880	0.0	20	0.3
4880-5150	-0.049	40	-0.8
5150-5450	0.065	30	2.0
5450-8360	-0.038	25	-0.6
8360-8910	0.076	35	2.3

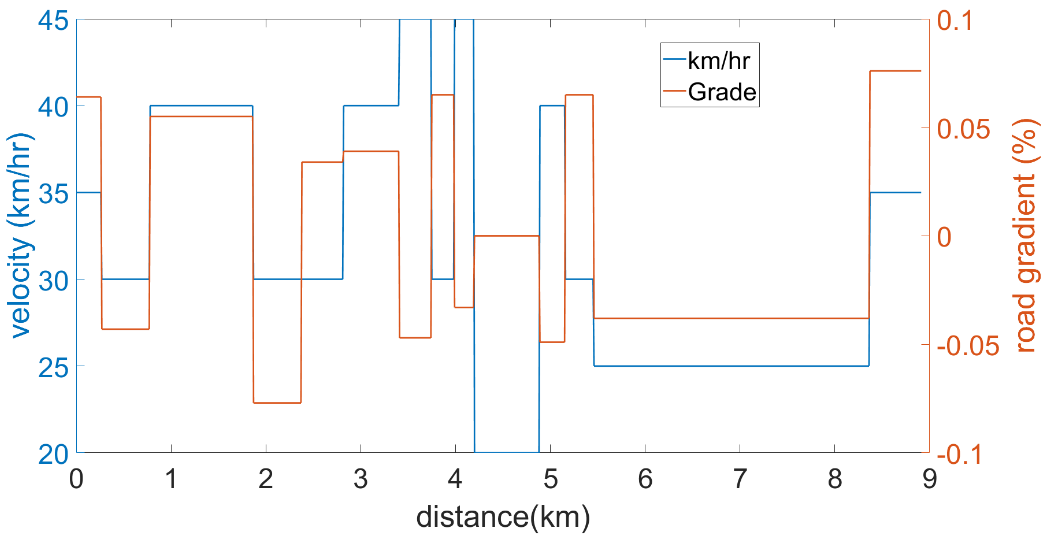

Figure 6.5: eBus optimal speed for the whole drive route

The speed curve in Fig. 6.5 does not include acceleration and traffic jams or stops. It is merely a guide to the driver on which speed to follow in order to save energy on that driving range whenever possible according to road traffic and safety. Fig.6.6 shows different motoring consumption rates versus road gradients of different drive

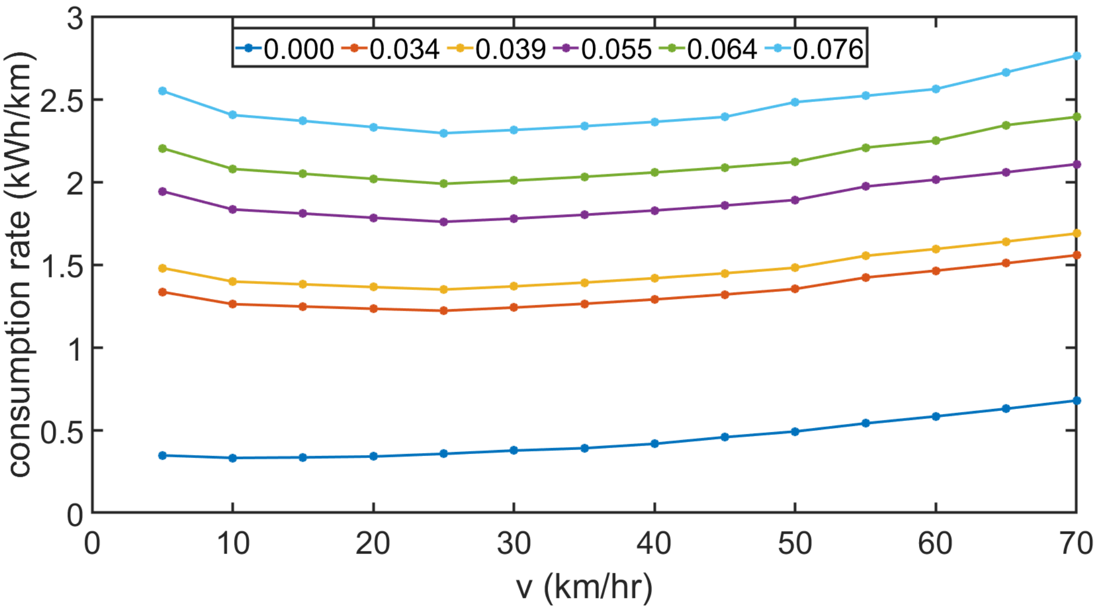

Figure 6.6: kWh/km for different road grades

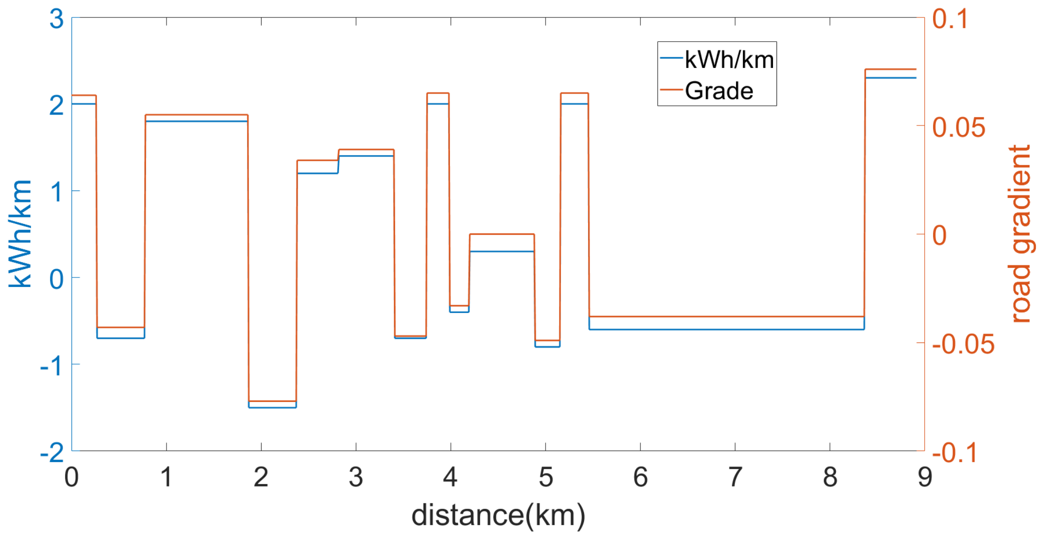

Figure 6.7: Consumption rate vs. road gradient

ranges. It is evident from the curves in Fig. 6.6, that the higher the road gradient, the higher the energy consumption rate, especially at higher eBus speeds. This is as a result of immense torque increment due to the climbing force because $sin\theta$ increases between $0°$ and $45°$. And the spike due to v^2 in the aerodynamic force term. On the contrary, the efficiency is on a declining trend during high speeds and higher torque regions as it is clearly noticeable on the efficiency map in Fig. 6.1. Therefore, it can be generally stated that a route with a gentle gradient for the

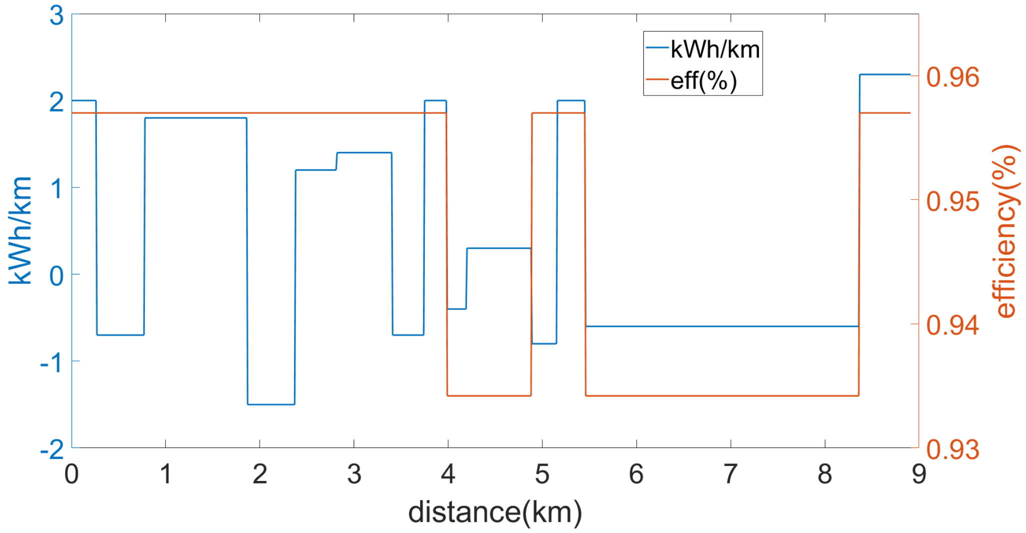

Figure 6.8: Consumption rate vs. efficiency

same origin and destination can decrease battery energy consumption as compared to a steeper alternative path, particularly, if the EV is driven at optimal speed. Fig. 6.6 also reveals that for the $8360 - 8910$m drive range with a road grade of 0.076, the consumption rate at 5km/hr is exactly the same as the consumption rate at 60km/hr which is 2.6kWh/km. This is mainly because at 5km/hr (173rpm) the efficiency is still low whereas at 60km/hr (2077rpm) the energy consumption is significantly influenced by the increase in aerodynamic force due to the v^2 term plus the climbing force. Thus, it is paramount to drive with an optimal speed especially in steeper roads. The consumption rate characteristics curves in Fig. 6.6, suggest that driving at low speeds ($\leq$ 15km/hr) is a very bad idea for this traction motor as it has a poor efficiency at lower speeds and high torque regions as shown by the efficiency map in Fig. 6.1. Driving the eBus at higher speeds ($\geq$ 55km/hr) and higher torque is very detrimental to energy consumption rate due to poor efficiency of the traction machine combined with large aerodynamic forces. Traction motor efficiency during this region would have already surpassed its climax efficiency of 95.7%. Fig. 6.6 can be extrapolated to estimate the consumption rates of other road grades without the use of the efficiency map. This is because the shapes of the characteristic curves of the different road grades are congruous to each other, but only have a mere difference due to the climbing force $mgsin\theta$ term in between them. And mathematically, $sin\theta \approx\theta$, for -0.2441$\leq$ θ $\geq$ 0.2441 rads, which hints that the difference between the curves can even be approximated with a linear factor for small angles.

Fig. 6.7 and Fig. 6.8 shows consumption rate versus road gradient and motor efficiency, respectively. It can be seen that much of the motoring optimum consumption rates occur during motor efficiency of 95.7% which is the possible maximum efficiency. But the zero gradient motoring optimum consumption rate and the optimum regeneration rates i.e (-0.033 and -0.038 road grades) occur at 93.42% which is the second highest efficiency. The curves of Fig. 6.7 also captures the fact that energy consumption rate is higher for steeper road grades. It can be deduced that energy consumption rate and road grade are synchronous to each other. But this is mainly dependent on the shape and structure of the contours on the efficiency map.

From Table 6.2, it is observed that the optimal speeds fluctuate between 20-45km/hr which appears to be low as compared to the current speeds of the ICE buses for the all-residences route. Consequently, the eBus would take a longer time to complete the all-residences route as compared to current ICE buses. In such an event, firstly, this problem can be resolved by right shifting and widening the band of the most optimal contour (95.7%) on the efficiency map during the design process of the traction motor. The optimal speeds range could also be improved by using a traction machine that has a higher maximum efficiency i.e $\approx$ 98%. Therefore, it would be very helpful to design the traction motor for a specific drive cycle so that the motor efficiency can be pushed to its limits as this can definitely improve the mileage coverage in that particular closed-circuit route. Secondly, optimal speeds can be improved by an efficient aerodynamic drag coefficient C_d and small frontal area A_f. These two factor heavily depend on the shape and dimensions of the eBus. An efficient C_d and smaller A_f suppress the effect of the v^2 term and thus enhance an improvement on the optimal speed. To avoid all such problems, the eBus Simulink model needs to be simulated on the drive route prior to its purchase. This is a very vital procedure because an excellent correlation between the C_d, A_f and the shape of the efficiency map can be exploited to determine the required optimal speeds for a drive cycle.

6.3.3 Case Study A: Eco-driving versus Convectional Driving

The eco-driving strategy that is studied in this research only considers constant velocities yet the drive route under study is predominantly a stop-and-go (i.e traffic lights, stop signs,traffic jam) in nature. This proved to be a challenge on how to verify the benefits of eco-driving strategy in this study scenario. Thus, the $8360-8910$m drive range with a slope gradient of 0.076 was chosen for an eco-drive versus a convectional drive for the simulations. The $8360-8910$m drive range does not have traffic lights and traffic congestion especially in the evening. Under these traffic conditions, the bus is able to accelerate and reach a cruise velocity with less perturbations within a short period of time. And moreover, this drive range is the steepest throughout the whole journey. Since the current buses are not electric buses a velocity profile of the ICE bus from this drive range was measured and then used in the simulation of the eBus Simulink model. The convectional speed consumption rate is then compared to the optimal speed consumption rate. From Table 6.2, the optimal velocity of this drive range is 35km/hr with a consumption rate of 2.3kWh/km. The measured constant velocity that was achieved by the ICE bus was 50km/hr and this yielded a consumption rate of 2.5kWh/km on the eBus. Thus, the energy-saving drive strategy is able to decrease the consumption rate of the $8360 - 8910$m drive range by 8.7%. A route map with respective optimal velocities for all the drive ranges is shown in Fig. 6.3. This can be used by the driver to follow as much as possible depending on traffic conditions.

6.3.4 Case Study B: Extra-urban Driving

Case study B considers the Rosebank drive schedule and it has the following bus stops: Wits Junction>>Rosebank>>Wits Junction. This route has less stop and go components by nature as the bus is able to partly drive on the highway as well. Rosebank route also experience less traffic jams as it is only used during the weekends, thus it has a good representation of an extra-urban drive. Unlike in case study A, the bus can be able to reach higher speeds on this route. Fig. 6.9 shows the elevation profile of the Rosebank bus route.

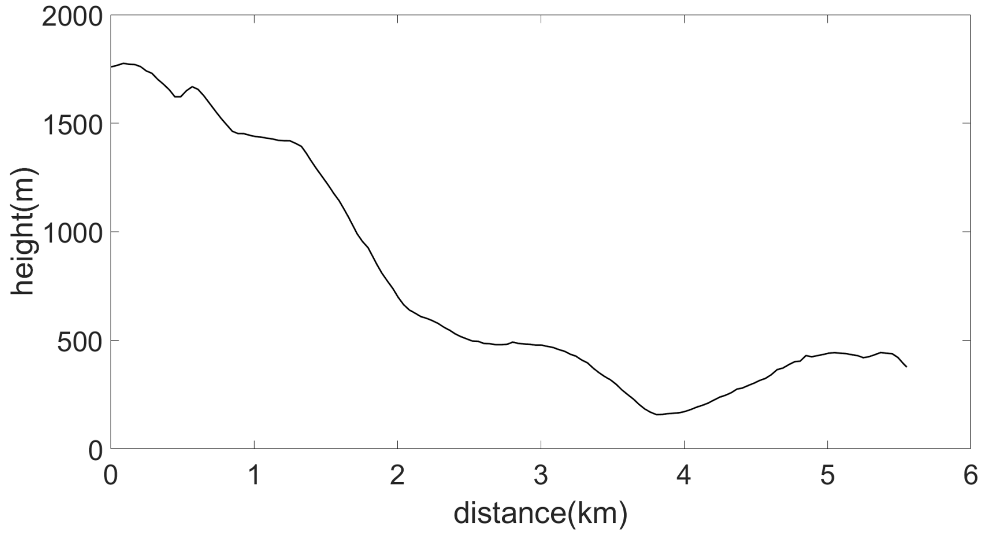

Figure 6.9: Case study B: elevation profile of the drive route

6.3.5 Case study B: Results Analysis and Discussion

Unlike in case study A, the Rosebank route has longer drive ranges which also have road grades that are not widely spread from each other as it can be observed in Fig. 6.9 and Table 6.3. Table 6.3 shows the simulation results of this drive schedule according to their respective drive ranges and road grades. For about 50% of the whole journey, the eBus can recuperate kinetic energy through regenerative braking if driven at desired optimal speeds. Analytically, Table 6.3 gives a total of 6.35kWh of motoring energy and a total of -2.36kWh of regeneration energy.

Table 6.3: Case study B: Drive range, gradients, optimal speed and consumption

drive range(m)	gradient(decimal)	Opt. km/hr	kWh/km
0-2500	-0.044	35	-0.7
2500-3850	-0.023	40	-0.2
3850-5530	0.021	35	0.9
5530-7210	-0.021	25	-0.2
7210-8560	0.023	45	1
8560-11060	0.044	40	1.4

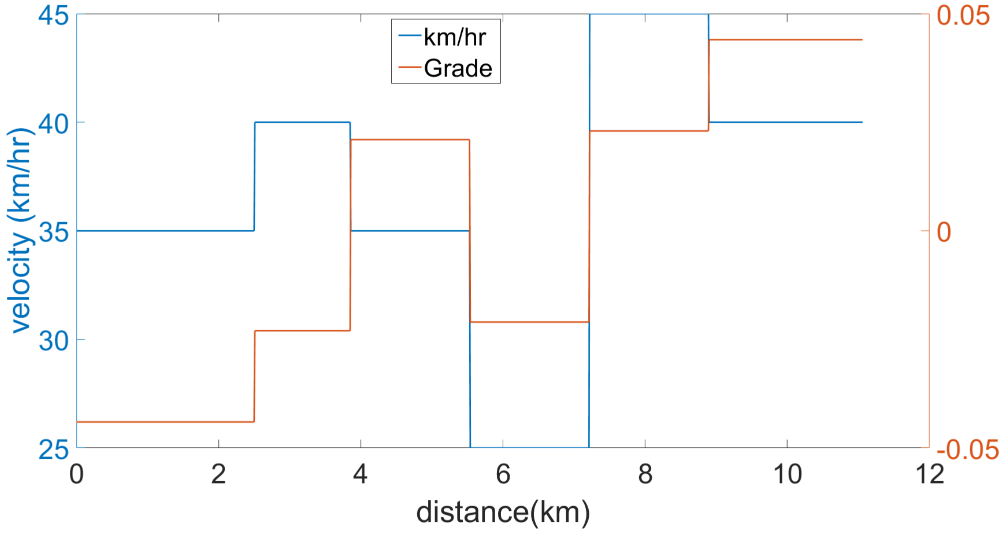

Figure 6.10: Case study B: eBus optimal speed for the whole drive route

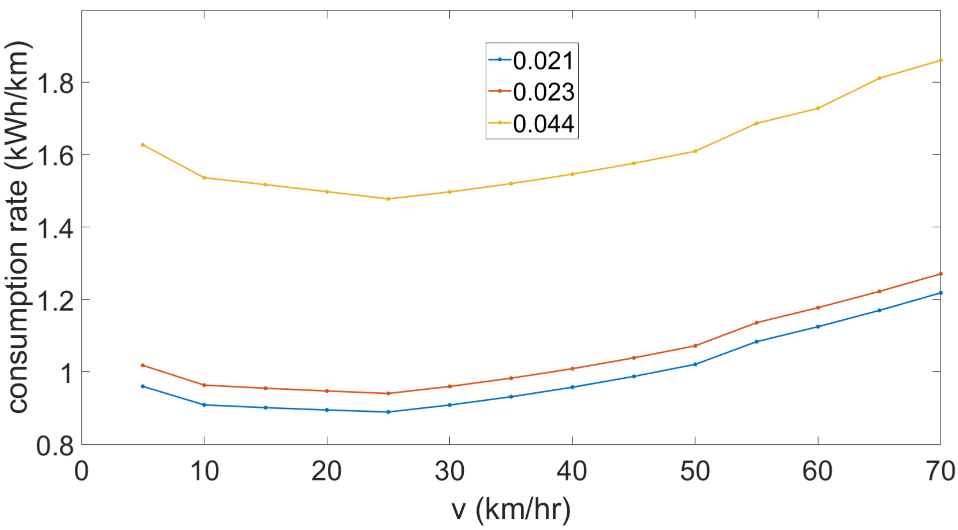

Figure 6.11: Case study B:kWh/km for different road grades

Taking a difference between the two suggest that this journey only needs 3.99kWh. This highlights the importance of optimal speed driving in order to elongate the mileage coverage of the EV. The optimal speeds in Table 6.3 were summed up together according to their respective road grades into an optimal speed that represents the whole journey as shown in Fig. 6.10. In an attempt to really improve energy consumption rate in this journey, Figs. 6.10, 6.12 and 6.13 could be used to train the bus drivers in order for them to follow the optimal velocities as much as possible. In such trainings, the bus drivers could get to understand the energy savings if they drive according to the optimal speed of a particular drive

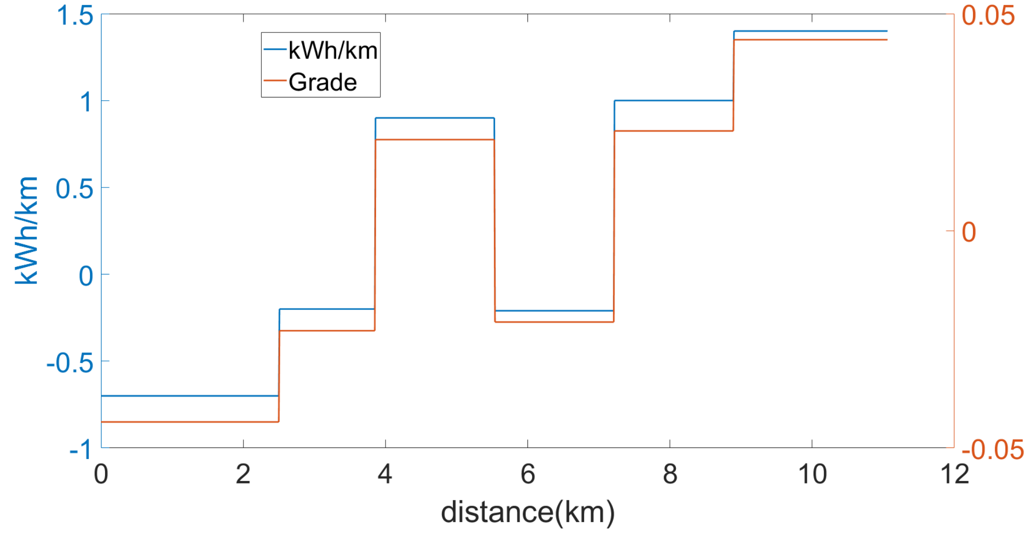

Figure 6.12: Case study B:consumption rate vs. road gradient

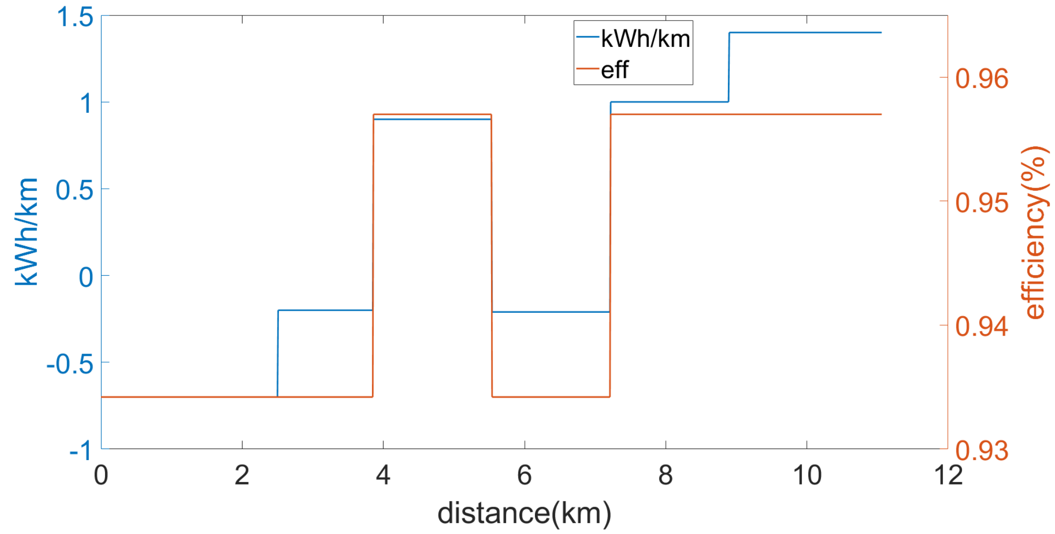

Figure 6.13: Case study B: Consumption rate vs. efficiency

range and road grade as compared to convectional driving. Fig. 6.11 shows the motoring consumption rates of the bus for all the three grades. Like in case study A, the highest road gradient consumes more energy especially during higher bus speeds. For the 0.044 road grade, the bus has a consumption rate of 1.6kWh/km at 5km/hr and 1.9kWh/km at 70km/hr. Driving the bus at the optimal speed of 40km/hr saves 14.3% of consumption energy as compared to driving at 5km/hr. A saving of 35.7% is yielded by driving the bus at 40km/hr as compared to 70km/hr. Fig. 6.12 and Fig. 6.13 show the optimal consumption rates versus road grade and efficiency, respectively. Figs. 6.12 and 6.13 suggest that a traction motor with a higher maximum efficiency i.e $\approx 98\%$ can lessen the higher consumption rates which are experienced on the higher road gradients.

6.3.6 Case Study B: Eco-driving versus Convectional Driving

Since there was less traffic flow during the measurements of the speeds attained by the ICE bus, all three motoring drive ranges are considered for the comparison between eco-driving and convectional driving as shown on Table 6.4. The eBus has a maximum speed of 70km/hr hence all the convectional energy consumption rates are for 70km/hr as according to Fig. 6.11. Even though the ICE bus attained much higher speeds on these respective drive ranges. A massive energy saving can be realised if the eBus is driven according to the optimal speeds as it can be observed on Table 6.4. Unfortunately, these results suggest that this motor is unsuitable for this kind of a drive cycle since the optimal speeds are too low as compared to the the current actual speeds, hence the trip time requirements will be unsatisfactory. Such a challenge can be solved by using a traction machine that has the highest efficiency contours located on mid-lower torque and higher speeds regions on the efficiency map.

Table 6.4: Case study B: Eco-driving versus convectional driving

drive range(m)	speed(km/hr)	kWh/km	Opt.kWh/km	(%) savings
3850-5530	80	1.21	0.90	34.44
7210-8560	90	1.27	1.00	27.00
8560-11060	90	1.86	1.40	32.90

6.4 eBus Energy-efficient Acceleration Strategy

In order to realise a complete effectiveness of eco-driving strategy for the eBus, firstly, an optimal speed must be determined for the particular drive range of a known road grade. Then, the second step is to efficiently accelerate the bus into the desired optimal speed and keep it constant at that optimal speed for the duration of the drive range. From Tables 6.2 and Table 6.3, it can be observed that the optimal speeds for this eBus vary between 20-45km/hr in both case studies. It is also clear from the efficiency map that all these motoring optimal speeds occur on the 95.7% efficiency contour which approximately lies between 700-1800rpm. This subsection is mainly concerned with how the bus can be efficiently accelerated into the optimal speeds. Fig. 6.14 shows the acceleration profiles for v_f=6m/s (21.6km/hr), v_i=0, t_f=10s and Fig. 6.15 shows their respective acceleration energy consumption rates.

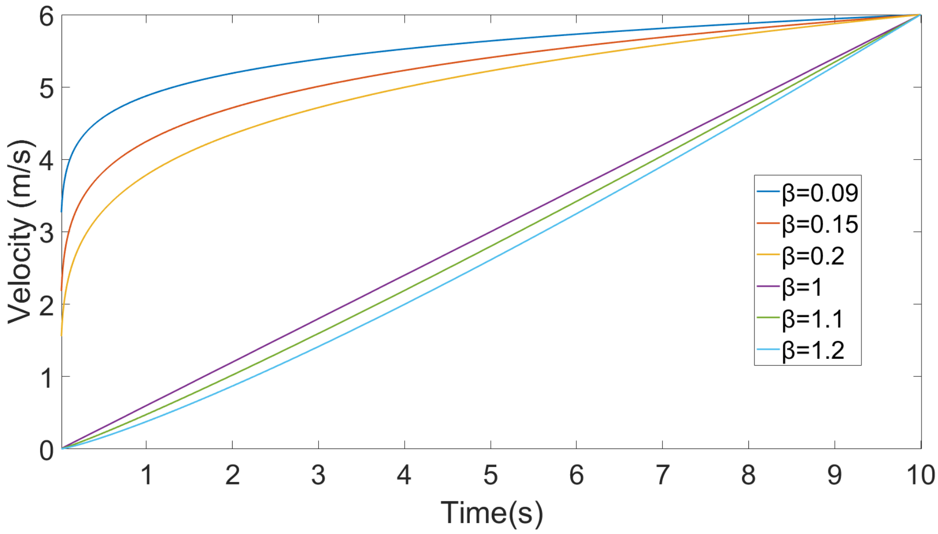

Figure 6.14: eBus acceleration characteristics curves

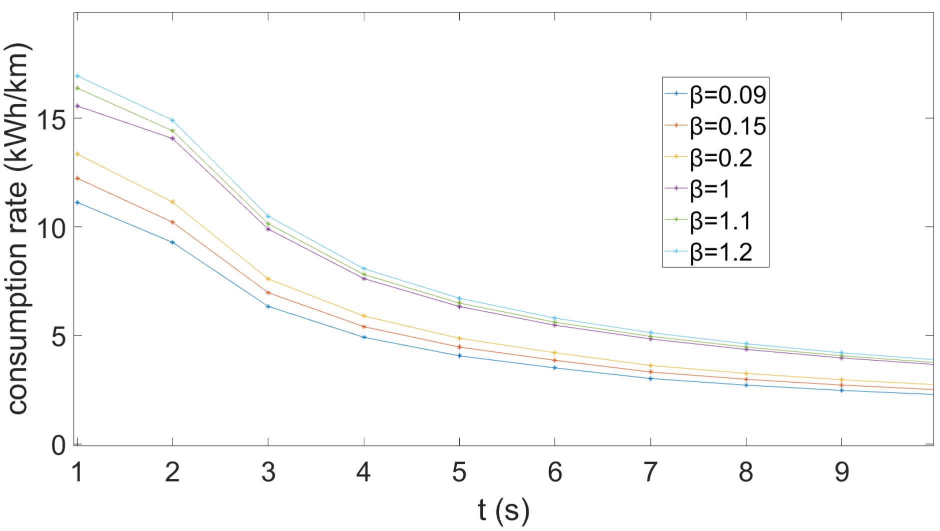

Figure 6.15: eBus acceleration consumption rates

Energy consumption rate increases with an increase in the acceleration characteristic β as shown in Fig. 6.15. This is for the accelerations from zero towards an optimal speed of 21.6km/hr as shown in Fig. 6.14. At higher torque and lower speeds the efficiency map has a poor efficiency region ($\leq$ 56%). It is clear from the efficiency map in Fig. 6.1 that the efficiency increases up until the 95.7% region which is the summit region of this efficiency map. The $\beta = 0.09$ acceleration mode is the most efficient acceleration architecture because it results in the bus reaching its optimal speed region quicker. In this way, the as-fast-as-possible acceleration style is the optimal mode to accelerate the bus from zero into any of these optimal speeds (20-45km/hr) and this concurs with the acceleration mode for TUM EV. The as-fast-as-possible acceleration mode requires the traction motor to have a very high torque capability in order to be able to thrust the bus into the optimal speeds region.

6.5 eBus Speedometer Interface

Electric vehicle OEMs can include an eco-drive module which interacts which with the bus driver through the speedometer as shown in Fig. 6.16. The eco-drive module implements the eco-driving strategy in the following chronological steps:

i. Use a global positioning system (GPS) to enter drive route information into the eco-drive module.

ii. Eco-drive module determines the eBus current GPS position and drive range and then calculates the required optimal speed .

iii. During the drive schedule, the bus should be accelerated with the as-fast-as-possible mode into the optimal speed i.e 35km/hr

iv. A beep must sound to alert the driver to stop the acceleration process

v. Driver should set the cruise controller into the required optimal speed

vi. Green LED lights should be illuminated so as to guidance to the driver

vii. Red LED lights should be illuminated on the speed ranges that has high energy consumption rates i.e 0-15km/hr and 55-70km/hr

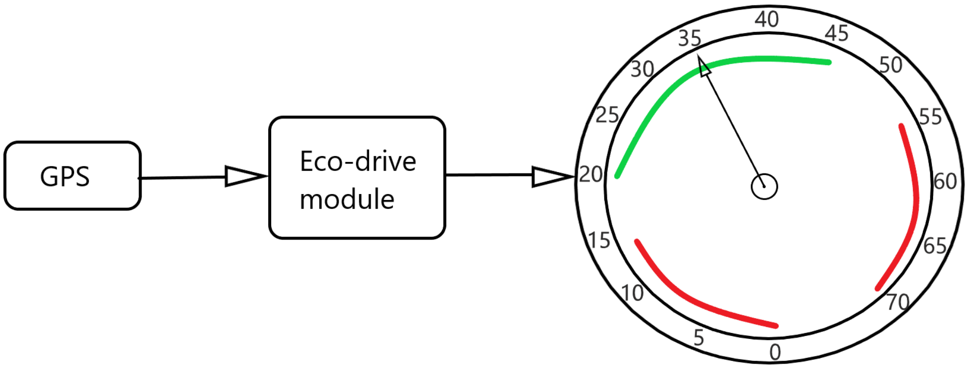

Figure 6.16: eBus speedometer

6.6 Summary

Application of the eco-driving strategy was implemented on the eBus in order to realise its benefits on a large-mass vehicle. Inter-campus routes for both an urban and an extra-urban driving were studied. It is recognized that for a constant road gradient, at lower eBus speeds ($\leq$ 15km/hr) energy consumption rate is high due to poor efficiency experienced at this region by the traction motor. Yet at mid-high speeds (45-60km/hr), the high energy consumption rate is due to the surge in aerodynamic drag force which is enforced by the quadratic v^2 term. It was recorded that at both higher road grade and higher speed energy consumption rate increased tremendously because of inadequate efficiency experienced by the traction machine in high torque and high speed regions. Eco-driving strategy was found to reduce energy consumption rate by 8.7% on the 8360-8910m drive range for a bus city drive. For extra-urban bus driving, there was a big difference between the optimal speeds and ICE bus actual speeds. Therefore, a traction motor which has the highest efficiency contours located on mid-lower torque and higher speeds region was recommended for an extra-urban drive. The as-fast-as-possible acceleration mode was found to be the most efficient acceleration mode to accelerate the eBus from zero or lower speeds towards the optimal speeds.

As a recap on EV eco-driving, firstly, it is important that during the EV procurement process, the EV end-user chooses the most influential technical parameters and traction motor properly. The most influential parameters are mass m, aerodynamic drag coefficient C_d, frontal area A_f and the traction motor efficiency. C_d, m and A_f systematically works together with the motor efficiency to determine the desired optimal speed and an efficient acceleration style. An efficient C_d, a moderate m, a small A_f and a traction machine with an efficiency map that is characterised by a wide region for the highest efficiency contours coupled with a very high torque capability are idealistic for lower energy consumption rates. Secondly, it is crucial to drive the EV at its optimal speed during a drive schedule, more especially on drive routes which have higher road grades. This is because at lower speeds the efficiency is poor therefore results into high energy consumption rates. Yet at higher speeds, the aerodynamic force surges whilst the traction motor operates on lower efficiencies. Thirdly, it is so essential to efficiently accelerate the EV to the optimal speed and then keeping constant on that optimal speed for the rest of the drive range. This is to avoid energy consumption due to inertia, especially for large-mass vehicles.

CHAPTER 7

Conclusion and Future Work

7.1 Conclusions

This section will provide a summary of the research done and its contributions.

7.1.1 Chapter 3

Vehicle dynamics together with vehicle technical parameters and factors that affect battery energy consumption in electric vehicles were reviewed from the literature. A general EV setup and the components in an EV were also considered. These included a short survey on common traction motors currently used in the EV industry and their typical requirements. A performance index for the Li-ion battery technologies and a checkup on the different EV powertrain configurations were conducted.

7.1.2 Chapter 4

This chapter was concerned with the validation of the Simulink EV model. A Simulink EV model that uses a PID controller as a driver is developed by mathematically modeling the kinematic equations of an electric vehicle. The Simulink EV model is able to determine the motor mechanical torque, speed, power, and energy consumption on the motor shaft. The Simulink EV model is also able to calculate the acceleration, velocity, and distance of the vehicle's motion. The efficiency map of an IPMSM traction machine is utilized to translate the mechanical energy consumption on the motor shaft into the input electrical energy from the battery supply. A measured drive cycle from the TUM EV was used to simulate the Simulink EV model. Firstly, an observation is made to see if the PID controller driver is able to follow and track the measured drive cycle. This is as a measure to make sure if the parameters of the PID controller were set properly. Secondly, a comparison in terms of energy consumption for the measured drive cycle between the TUM EV and Simulink EV model is conducted as means to validate the Simulink EV model. An error of 1.8% between the Simulink EV model and TUM EV was realized.

7.1.3 Chapter 5

An EV eco-driving strategy that is composed of optimal speed driving and energy-efficient acceleration strategies are separately designed, implemented, and validated. Optimal speed driving strategy is predominantly based on vehicle constant speed driving for a driving range with a known road grade. Energy-efficient acceleration strategy largely depends on the shape of the efficiency contours on the efficiency map and on whether the vehicle is being accelerated in a fast rate mechanism or a constant rate mechanism or a slow rate mechanism. The eco-driving strategy is simulated with the Simulink EV model then the TUM EV is driven likewise in order to validate the driving strategy. TUM EV was found to have an optimal speed of 24km/hr for zero gradient road and an error of 1.93% was realized in terms of energy consumption rate between TUM EV and the Simulink EV model. An energy saving of up to 31.2% is achieved when TUM EV is eco-driven as compared to conventional driving. The as-fast-as-possible acceleration mode ($\beta = 0.4$) was observed to yield less acceleration consumption energy rate for TUM EV acceleration from zero speed towards the optimal speed.

7.1.4 Chapter 6

The eco-drive strategy is deployed on an electric bus which is a large-mass vehicle and its urban and extra-urban drive applications are investigated. At high road grades and high vehicle speeds, the energy consumption rate exponentially rises. The EV needs to be efficiently accelerated to attain the optimal speed of the driving range and then driven constantly at the optimal speed for the rest of that driving range. Technical parameters and the type of traction machine should be chosen carefully before the procurement of the EV and then the EV should be eco-driven in order to realize sizeable mileage extension, thus can contribute to the switch from ICE to EV. An eco-driven eBus was able to have an energy-saving of 8.7% on a 550m drive range with a road gradient of 0.076.

7.2 Future Work

This research study was concerned with the issue of an eco-driving strategy for electric vehicles in an attempt to elongate their mileage coverage. It was observed that if the EV is driven either at lower speeds or higher speeds other than the optimal speed, there are higher energy consumption rates largely due to the efficiency map of the traction machine and road gradient. To further improve on energy consumption rate the following investigations are recommended:

i. Research on a methodology for design specific in traction motors for closed-circuit drive cycles.

ii. Investigate how kinetic energy recovery systems can be used to inject energy into the EV during poor efficiency regions of the efficiency map i.e during acceleration.

References

[1] TQ, "Servo-kits ilm85x13," https://www.tq-group.com/en/products/tq-robodrive/servo-kits-brakes-and-sensors/ilm85x13/, 2021.

[2] Y. Zhang, W. Yuan, R. Fu, and C. Wang, "Design of an energy-saving driving strategy for electric buses," *IEEE Access*, vol. 7, pp. 157 693–157 706, 2019.

[3] H. Heisler, *Advanced vehicle technology.* Elsevier, 2002.

[4] B. Ballinger, M. Stringer, D. R. Schmeda-Lopez, B. Kefford, B. Parkinson, C. Greig, and S. Smart, "The vulnerability of electric vehicle deployment to critical mineral supply," *Applied Energy*, vol. 255, p. 113844, 2019.

[5] T. Raczek, "The paris declaration on electro-mobility and climate change and call to action," https://unfccc.int/news/the-paris-declaration-on-electro-mobility-and-climate-change-and-call-to-action, 2015.

[6] C. Sundström, A. Voronov, O. Lindgärde, and A. Lagerberg, "Optimal speed and gear shift control of long-haulage trucks," *IFAC-PapersOnLine*, vol. 52, no. 5, pp. 471–477, 2019.

[7] L. Thibault, G. De Nunzio, and A. Sciarretta, "A unified approach for electric vehicles range maximization via eco-routing, eco-driving, and energy consumption prediction," *IEEE Transactions on Intelligent Vehicles*, vol. 3, no. 4, pp. 463–475, 2018.

[8] Y. Parvin, "Modeling, hybridization, and optimal charging of electrical energy storage," *Clemson Unversity, Dissertation*, 2016. [Online]. Available: https://tigerprints.clemson.edu/all_dissertati\ons/1709

[9] P. Kadav and Z. D. Asher, "Improving the range of electric vehicles," in *2019 Electric Vehicles International Conference (EV)*, 2019, pp. 1–5.

[10] H. Laitinen, A. Lajunen, and K. Tammi, "Improving electric vehicle energy efficiency with two-speed gearbox," in *2017 IEEE Vehicle Power and Propulsion Conference (VPPC)*. IEEE, 2017, pp. 1–5.

[11] Y. Guan, Z. Q. Zhu, I. A. A. Afinowi, J. C. Mipo, and P. Farah, "Design of synchronous reluctance and permanent magnet synchronous reluctance machines for electric vehicle application," in *2014 17th International Conference on Electrical Machines and Systems (ICEMS)*, 2014, pp. 1853–1859.

[12] B. A. Aderemi, A. T. Puati Zau, S. D. Chowdhury, T. O. Olwal, and A. M. Abu-Mahfouz, "Hybrid battery technologies with battery management system in power and energy sectors," in *2018 IEEE PES/IAS PowerAfrica*, 2018, pp. 716–721.

[13] W. F. Infante, A. F. Khan, N. J. C. Libatique, G. L. Tangonan, and S. N. Y. Uy, "Performance evaluation of series hybrid and pure electric vehicles using lead-acid batteries and supercapacitors," in *TENCON 2012 IEEE Region 10 Conference*, 2012, pp. 1–5.

[14] R. Karangia, M. Jadeja, C. Upadhyay, and H. Chandwani, "Battery-supercapacitor hybrid energy storage system used in electric vehicle," in *2013 International Conference on Energy Efficient Technologies for Sustainability*, 2013, pp. 688–691.

[15] D. J. Goss, "Performance analysis of electric motor technologies for an electric vehicle powertrain." Motor design limited, 2019, accessed: 17/03/2020. [Online]. Available: https://www.motor-design.com/resource/performance-analysis-of-electric-motor-technologies-for-an-electric-vehicle-powertrain/

[16] E. Paul, N. Paulson, R. Bijoy, and B. KK, "Wireless charging of electric vehicles," *International Research Journal of Engineering Technology*, vol. 6, no. 6, 2019.

[17] R. Wang, Y. Chen, D. Feng, X. Huang, and J. Wang, "Development and performance characterization of an electric ground vehicle with independently actuated in-wheel motors," *Journal of Power Sources*, vol. 196, no. 8, pp. 3962–3971, 2011. [Online]. Available: https://www.sciencedirect.com/science/article/pii/S037877531002152X

[18] X. Yuan, J. Wang, and K. Colombage, "Torque distribution strategy for a front and rear wheel driven electric vehicle," 2012.

[19] H. Fujimoto and S. Harada, "Model-based range extension control system for electric vehicles with front and rear driving–braking force distributions," *IEEE Transactions on Industrial Electronics*, vol. 62, no. 5, pp. 3245–3254, 2015.

[20] J. Gonder, M. Earleywine, and W. Sparks, "Analyzing vehicle fuel saving opportunities through intelligent driver feedback," *SAE International Journal of Passenger Cars-Electronic and Electrical Systems*, vol. 5, no. 2012-01-0494, pp. 450–461, 2012.

[21] M. Sivak and B. Schoettle, "Eco-driving: Strategic, tactical, and operational decisions of the driver that influence vehicle fuel economy," *Transport Policy*, vol. 22, pp. 96–99, 2012.

[22] D. Shen, D. Karbowski, and A. Rousseau, "A minimum principle-based algorithm for energy-efficient eco-driving of electric vehicles in various traffic and road conditions," *IEEE Transactions on Intelligent Vehicles*, vol. 5, no. 4, pp. 725–737, 2020.

[23] X. Lin, D. Görges, and S. Liu, "Eco-driving assistance system for electric vehicles based on speed profile optimization," in *2014 IEEE Conference on Control Applications (CCA)*, 2014, pp. 629–634.

[24] G. P. Padilla, S. Weiland, and M. C. F. Donkers, "A global optimal solution to the eco-driving problem," *IEEE Control Systems Letters*, vol. 2, no. 4, pp. 599–604, 2018.

[25] D. Shen 1a, D. A. Karbowski, and A. Rousseau, “Highway eco-driving of an electric vehicle based on minimum principle,” in *2018 IEEE Vehicle Power and Propulsion Conference (VPPC)*, 2018, pp. 1–8.

[26] H. Laitinen, A. Lajunen, and K. Tammi, “Improving electric vehicle energy efficiency with two-speed gearbox,” in *2017 IEEE Vehicle Power and Propulsion Conference (VPPC)*, 2017, pp. 1–5.

[27] P. Dalrymple and R. Griffiths, “Force, mass and acceleration,” *Anaesthesia & Intensive Care Medicine*, vol. 6, no. 9, p. 294, 2005.

[28] Z. Hui, W. Jia, and Y. Zhigang, “Numerical analysis on effect of vehicle length on automotive aerodynamic drag,” 2012.

[29] S. F. T. S. M. A. Willem Toet, Head of Aerodynamics, “Aerodynamics of f1,” https://www.formula1.com, 2021.

[30] G. R. Center, “National aeronautics and space administration,” https://www.grc.nasa.gov/www/k-12/airplane/shaped.html, 13 May 2021.

[31] J. Katz, “Aerodynamics of race cars,” *Annu. Rev. Fluid Mech.*, vol. 38, pp. 27–63, 2006.

[32] C. E. Anne Marie Helmenstine, Ph.D., “What is the density of air at stp?” https://www.thoughtco.com/density-of-air-at-stp-607546, 4 February 2020.

[33] G. Di Leo, C. Liguori, A. Ruggiero, D. Russo, and P. Sommella, “Accurate measurement of kinetic friction coefficient by using two types of tribometer,” in *2019 IEEE International Instrumentation and Measurement Technology Conference (I2MTC)*. IEEE, 2019, pp. 1–6.

[34] Michelin, “michelin-ultimate-energy-tire,” https://thetiredigest.michelin.com/michelin-ultimate-energy-tire/, 2021.

[35] A. M. Lulhe and T. N. Date, “A technology review paper for drives used in electrical vehicle (ev) & hybrid electrical vehicles (hev),” in *2015 International Conference on Control, Instrumentation, Communication and Computational Technologies (ICCICCT)*. IEEE, 2015, pp. 632–636.

[36] M. Popescu, J. Goss, D. A. Staton, D. Hawkins, Y. C. Chong, and A. Boglietti, "Electrical vehicles—practical solutions for power traction motor systems," *IEEE Transactions on Industry Applications*, vol. 54, no. 3, pp. 2751–2762, 2018.

[37] I. Bolvashenkov, J. Kammermann, S. Willerich, and H.-G. Herzog, "The choice of electric traction motors for a helicopter traction drive."

[38] T. A. Huynh and M.-F. Hsieh, "Performance analysis of permanent magnet motors for electric vehicles (ev) traction considering driving cycles," *Energies*, vol. 11, no. 6, p. 1385, 2018.

[39] M. Popescu, N. Riviere, G. Volpe, M. Villani, G. Fabri, and L. di Leonardo, "A copper rotor induction motor solution for electrical vehicles traction system," in *2019 IEEE Energy Conversion Congress and Exposition (ECCE)*. IEEE, 2019, pp. 3924–3930.

[40] B. University, "Types of lithium batteries," https://batteryuniversity.com/article/bu-205-types-of-lithium-ion, 2021.

[41] Y. Miao, P. Hynan, A. Von Jouanne, and A. Yokochi, "Current li-ion battery technologies in electric vehicles and opportunities for advancements," *Energies*, vol. 12, no. 6, p. 1074, 2019.

[42] M. Wentker, M. Greenwood, and J. Leker, "A bottom-up approach to lithium-ion battery cost modeling with a focus on cathode active materials," *Energies*, vol. 12, no. 3, p. 504, 2019.

[43] P. A. Nelson, K. G. Gallagher, I. D. Bloom, and D. W. Dees, "Modeling the performance and cost of lithium-ion batteries for electric-drive vehicles - second edition." [Online]. Available: https://www.osti.gov/biblio/1209682

[44] B. A. Aderemi, A. T. P. Zau, S. D. Chowdhury, T. O. Olwal, and A. M. Abu-Mahfouz, "Hybrid battery technologies with battery management system in power and energy sectors," in *2018 IEEE PES/IAS PowerAfrica*. IEEE, 2018, pp. 716–721.

[45] A. Lajunen, "Comparison of different powertrain configurations for electric city bus," in *2014 IEEE Vehicle Power and Propulsion Conference (VPPC)*. IEEE, 2014, pp. 1–5.

Appendix A

Case Study A: Consumption Rate Characteristics Curves

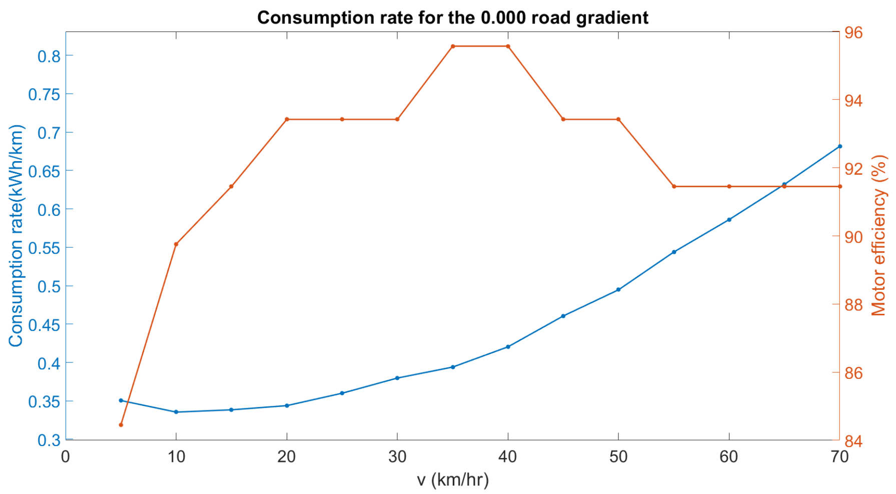

Figure A.1: Consumption rate for 0.000 road grade

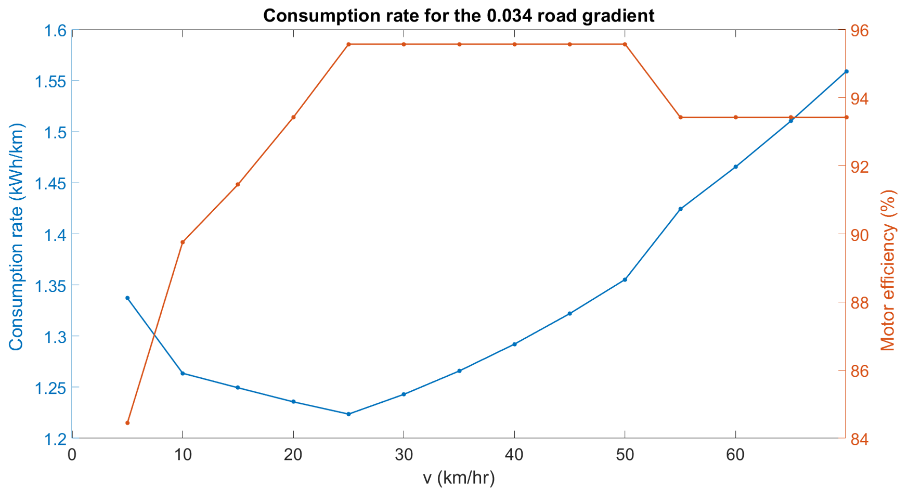

Figure A.2: Consumption rate for 0.034 road grade

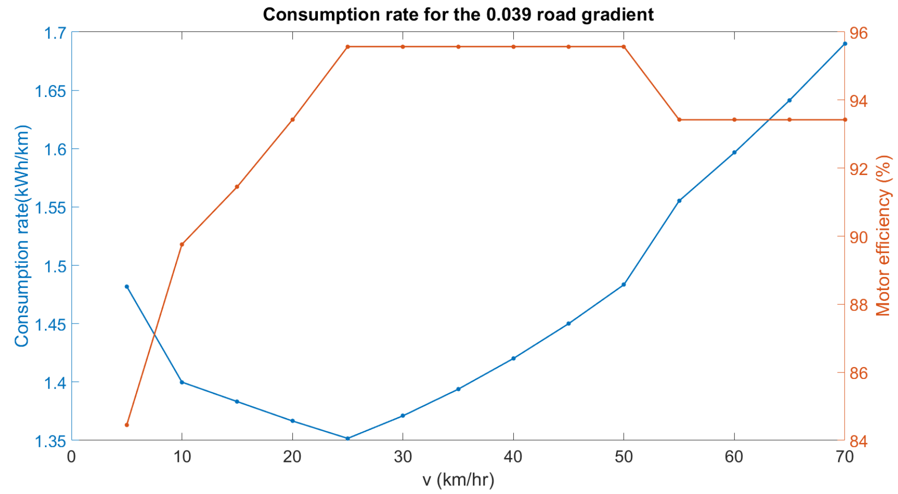

Figure A.3: Consumption rate for 0.039 road grade

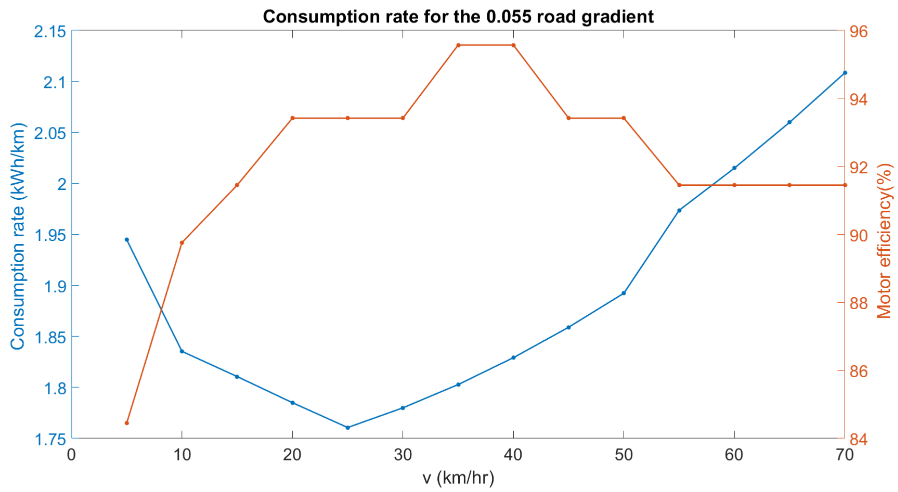

Figure A.4: Consumption rate for 0.055 road grade

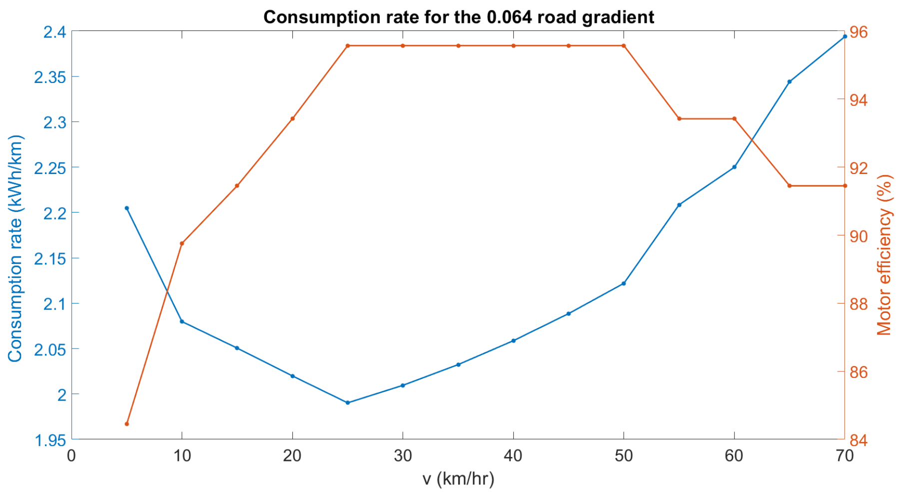

Figure A.5: Consumption rate for 0.064 road grade

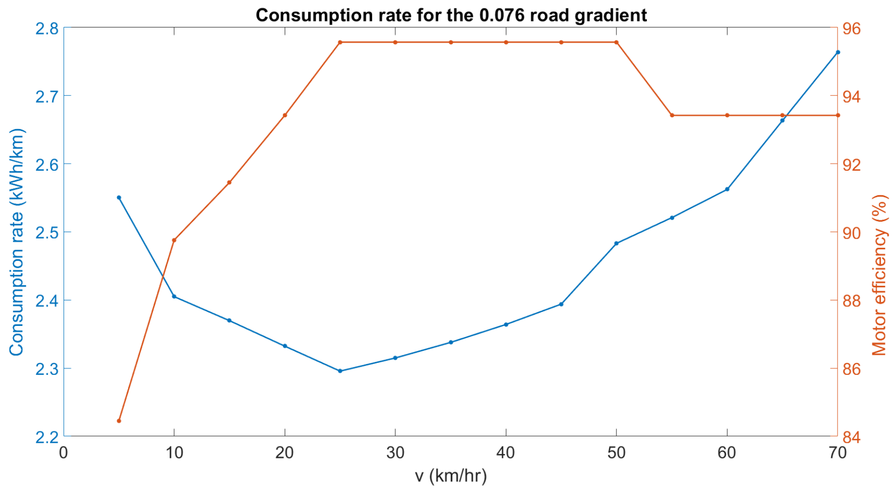

Figure A.6: Consumption rate for 0.076 road grade

Appendix B

Case Study B: Consumption Rate Characteristics Curves

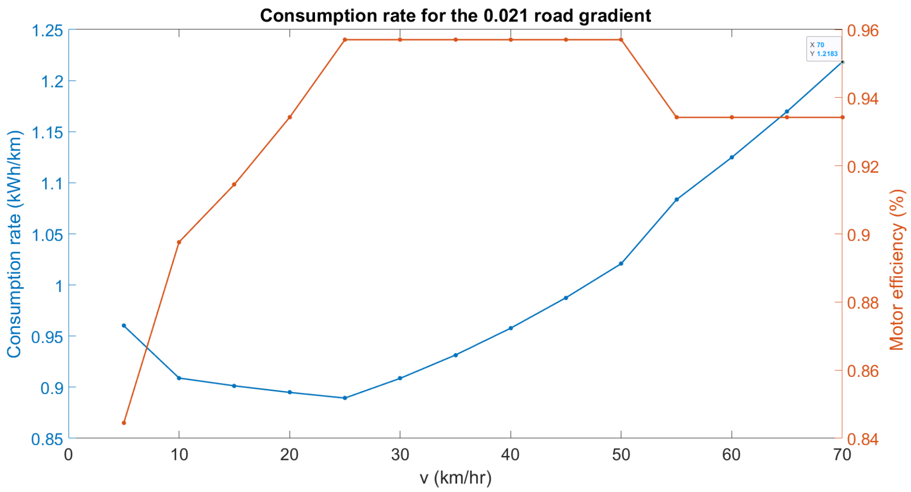

Figure B.1: Consumption rate for 0.021 road grade

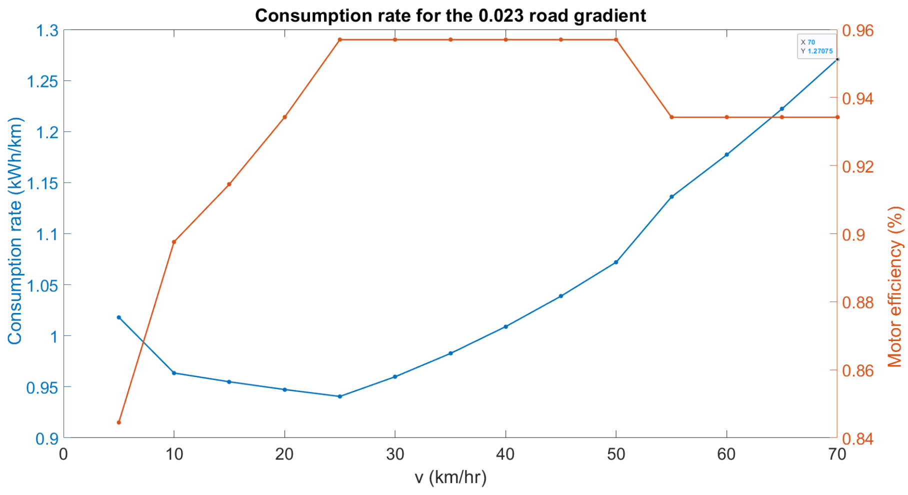

Figure B.2: Consumption rate for 0.023 road grade

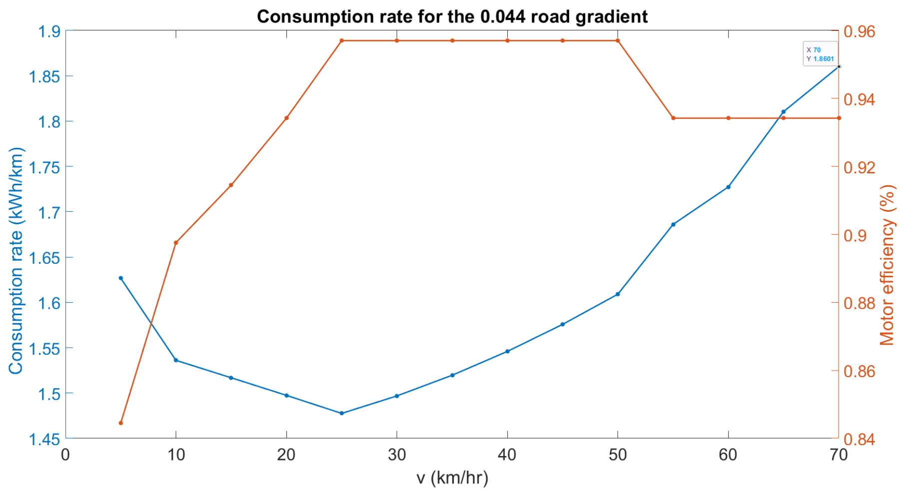

Figure B.3: Consumption rate for 0.044 road grade